NASA
Technical
Paper
3155

September 1991

NASA-TP-3155 19910021004

Equivalent Crystal Theory of Alloys

Guillermo Bozzolo
and John Ferrante

LIBRARY COPY
SEP 1 5 1991
LANGLEY RESEARCH CENTER
LIBRARY NASA
HAMPTON, VIRGINIA

NASA

NASA
Technical
Paper
3155

1991

Equivalent Crystal Theory of Alloys

Guillermo Bozzolo
Analex Corporation
Fairview Park, Ohio

John Ferrante
Lewis Research Center
Cleveland, Ohio

NASA
National Aeronautics and
Space Administration
Office of Management
Scientific and Technical
Information Program

Summary

Equivalent crystal theory (ECT) is a new semiempirical approach to calculating the energetics of solids with defects. The theory has successfully reproduced surface energies in metals and semiconductors. The theory of binary alloys, both with first-principle and semiempirical models, to date has not been extremely successful in predicting the energetics of alloys. This paper presents an extension of ECT, which is used to predict the heats of formation, cohesive energies, and lattice parameters of binary alloys of Cu, Ni, Al, Ag, Au, Pd, and Pt as functions of composition. This procedure accurately reproduces the heats of formation versus composition curves for a variety of binary alloys. The results are then compared with other approaches, such as the embedded atom method or Miedema's method. In addition, a new sum rule, which predicts the cohesive energies and lattice parameters of alloys from pure metal properties more accurately than Vegard's law, is presented.

Introduction

The equivalent crystal theory (ECT) (refs. 1 to 3), recently extended to include a proper treatment of bond length anisotropy and bond angle anisotropy (ref. 4), is still limited in its inability to treat systems with more than one atomic species. The basic idea underlying this theory, that is, the existence of an equivalent, fictitious crystal for each atom encompassing the range of a certain local defect, is not applicable to alloys, since the only difference between this fictitious single crystal and the actual ground state crystal is that its lattice constant differs from its ground state value. Thus, nothing in ECT accounts for a variety of atomic species in the local environment. In other words, an alloy cannot be considered as a defect of an otherwise pure crystal (i.e., a crystal of one atomic species).

Retaining the atomic identity of the constituents is essential in developing a technique for calculating alloy properties. Without atomic identity, detailed knowledge of the particular alloy properties we wish to predict would be required. Such particularity would limit the range of applicability of any method attempting to deal with multicomponent systems. To use the current version of ECT for alloys, it would be necessary to redefine the system, its components, and the formal perturbative series so that each atom would become an "average" alloy particle and so that the interactions with neighboring alloy particles would be redefined accordingly. However, to apply ECT directly, *a priori* knowledge is required of the structure and properties of that alloy with the lowest possible cohesive energy, which is clearly impossible as in most cases it is one of the pure components, and not the alloy, that is sufficiently well known. The values of the binding energy and cohesive energies are the same at the minimum in the binding energy curve when it is referenced to zero at infinite separation.

In deriving an alternative approach to an exact treatment of alloys (that, if satisfied, would allow for a simple and efficient study of alloys and defects), we face two constraints: (1) We must keep a single-species description, thus allowing us to treat individual atoms as building blocks of any metallic compound, and (2) we must be able to introduce specific alloy properties in a perturbative fashion to properly account for the behavior of multicomponent systems. Further, in order to retain the simplicity and numerical accuracy of the original ECT, we chose to base our approach on it.

In the original ECT, each atom in a defect crystal is assigned an equivalent crystal of the same atomic species. The lattice parameter of this equivalent crystal is determined such that the energy of an atom in the equivalent crystal is the same as the energy of the atom in the defect crystal. The lattice parameter of the equivalent crystal is obtained via a perturbative scheme which translates into solving a simple transcendental equation containing information about the nature of the defect. Once the equivalent lattice parameter is determined, the energy is computed by means of the universal binding energy relation. This energy is actually the difference in the energy of the atom in the defect crystal and that in the atom in the ground state crystal.

In an alloy, however, an atom of a given species finds itself in a different environment from the one in the ground-state pure crystal of its own species: the geometry is different, and some of the neighboring atoms are of a different species. These two changes should be dealt with separately, as they cannot both be considered defects. Within the framework of ECT, a defect is any change of the local environment of the pure crystal where nothing is necessarily conserved, except the identity of the atoms. The equivalent crystal of any given atom in the defect crystal is a compressed or expanded version of the ground-state pure crystal. In this sense, then, the formation of an alloy A–B cannot be considered as a "defect A" or "defect B" crystal.

The basic difference between the changes in geometry related to alloy formation (with reference to pure single crystals) and the composition effects, forces us to establish a procedure that will treat each aspect separately.

We now formulate a technique that maintains the simplicity of ECT and uses pure metal properties to calculate alloy properties. This procedure is then tested by comparing its predictions with experimental data, first-principles calculations, and other semiempirical and empirically based methods.

In the section on equivalent crystal theory we briefly review the fundamental ideas of the equivalent crystal theory for pure metals. In the section "Formalism" a detailed description of the new formalism is given. The following two sections give the results and an extended discussion which includes comparisons with other methods.

Symbols

a	equilibrium lattice constant, A
a_e	equilibrium lattice constant
B	equilibrium bulk modulus, GPa
c_1 (c_2)	ratio between nearest (next-nearest) neighbor distance and the lattice parameter
E	energy
E^{BA}, E^{AB}	heats of solution of impurity in host
E_c	cohesive energy, eV
ΔE_c	minimum total energy, i.e., the equilibrium binding energy, eV
$\Delta E_D(r,x)$	excess internal energy for disordered alloys
$E_m(r)$	binding energy of ordered alloy
$\Delta E_m(r_m)$	excess internal energy for ordered alloys
$E_m(r),E_x(r)$	binding energy curve for (dis)ordered compound
e_c^*	chemical energy (eq. (9))
e_s	strain energy
ΔH	heat of formation, the difference in energy between the constituent atoms of the compound at equilibrium and their composition-averaged bulk values in the pure crystals
j	identity of the neighbor of atom i located at a distance r_j from the host atom
l	screening length, $= (E_c/12\pi B r_{wse})^{1/2}$, A
l_A	scaling length
$N(M)$	nearest (next-nearest) neighbors
N_1 (N_2)	number of nearest and next nearest neighbors in a perfect (equivalent) crystal
n	principal atomic quantum number
$P(x)$	interpolating polynomial for heat of formation of disordered alloys
p	$= 2n - 2$
Q	arbitrary point on the binding energy curve of a certain crystal
R_1 (R_2)	nearest (next-nearest) neighbor distance in the perfect crystal (eq. (13))
r	lattice parameter
r_j	distance between j^{th} neighbor and atom under consideration
r_{wse}	equilibrium value of Wigner-Seitz radius
x	arbitrary concentration
α	parameter that will primarily reflect the structure of the electron density in the overlap region, parameter computed by requiring agreement with the experimental vacancy formation energy
Δ_{AB}, Δ_{BA}	perturbative parameters
Δ_m^∞	energy reference
λ	electronic screening length
$v_n(r)$	many-body interaction potentials
ξ	multisite correlation functions defined on an nth order cluster

Subscripts:

A	metal A
AB	impurity A in host B
B	metal B
BA	impurity B in host A
m	indicates ordered alloys
v	virtual crystal
x	indicates disordered alloys

Superscripts:

A	metal A
AB	impurity A in host B
B	metal B
BA	impurity B in host A

Equivalent Crystal Theory of Metal and Semiconductors

The equivalent crystal theory (ref. 4) is a new tool for the treatment of real material defects at the atomic level. The method treats surface energies and the surface relaxation of semiconductors and metals accurately. The basic idea of this method is that, for any crystal with a defect, an atom in the vicinity of the defect has the same energy that it would have in a certain perfect (equivalent) crystal, which we define later. The defect crystal can be formally described as a perturbation

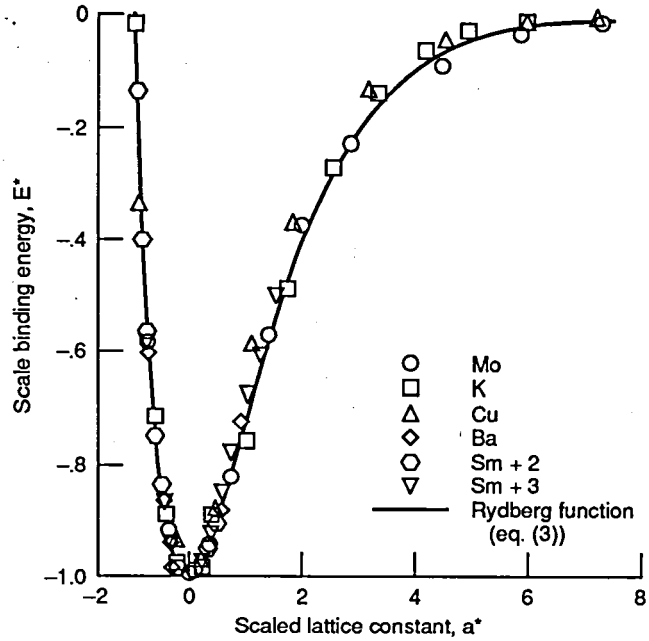

Figure 1.—Scaled binding energy per atom of a crystal as function of interatomic separation for representative solids. The sources for unscaled results are listed in ref. 12.

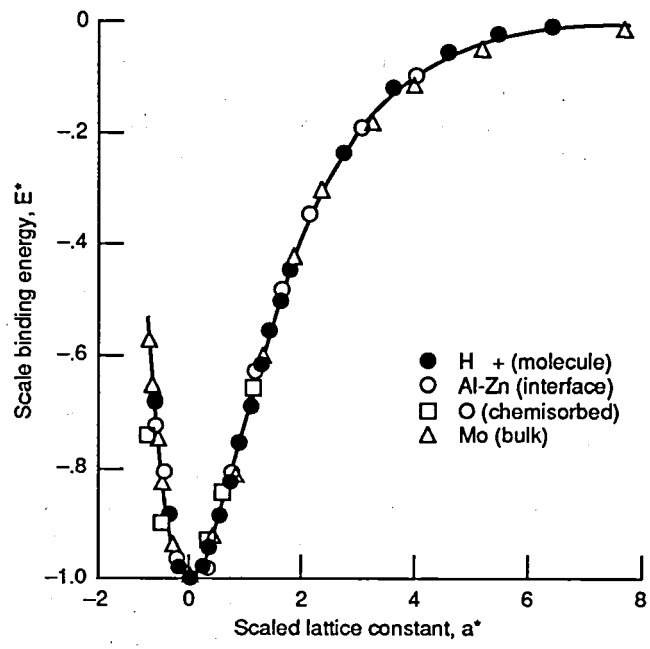

Figure 2.—Scaled binding energy versus scaled separation for representative cases of cohesion, bimetallic adhesion, chemisorption, and diatomic molecule. Sources of unscaled results are listed in ref. 12.

of a perfect crystal whose lattice parameter is chosen to minimize the perturbation.

The procedure is very simple, and for each atom near a defect, it involves solving a few transcendental equations that represent the perturbation between the real defect crystal and the perturbed, equivalent crystal. The number of equations depends on the complexity of the defect. The solution of these equations gives the lattice parameter of the equivalent crystal. In a straightforward calculation, each atom is then assigned its own equivalent crystal whose energetics follow a universal behavior given by the universal binding energy relation.

Total energies as a function of interatomic spacings have been discovered to have a single, universal form for bimetallic adhesion, for cohesion in metals (fig. 1), for metallic and covalent bonds in chemisorption, for many diatomic molecules (fig. 2), and even for nuclear matter. All these curves are scaled on to one universal form, which can be obtained by a simple scaling of the total energy:

$$E(a) = E_c E^*(a^*) \tag{1}$$

where

$$a^* = \frac{a - a_e}{l} \tag{2}$$

and where E_c is the minimum value of the total energy, that is, the equilibrium binding energy, and l is a conveniently defined scaling length. As shown in figures 1 and 2, a simple analytic form accurately represents the universal energy relation:

$$E^*(a^*) = -(1 + a^*) \exp - a^* \tag{3}$$

From the point of view of an individual atom in a certain crystal, each point of the binding energy curve can be interpreted in two different ways. To fix ideas, let's consider an arbitrary point Q on the binding energy curve of a certain crystal (fig. 3):

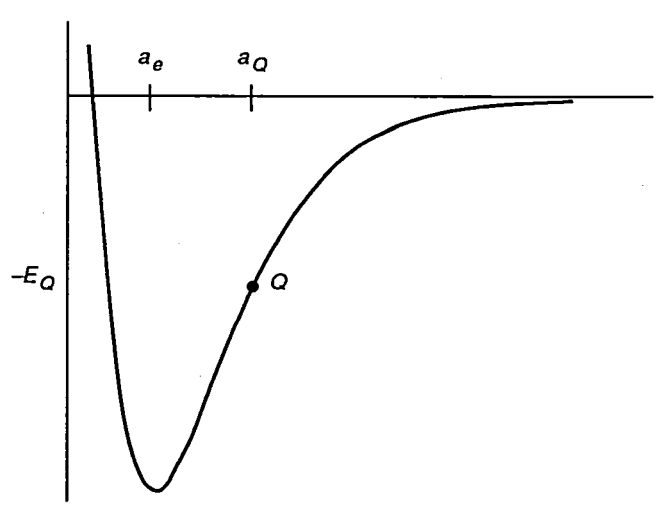

Figure 3.—Any point Q on binding energy curve.

Point Q then denotes (1) the energy E_Q of the atom when the perfect crystal is uniformly expanded until its lattice constant has the value a_Q, and (2) the energy E_Q of the atom in a defect crystal, but where the defect is such that its equivalent crystal has the same lattice constant a_Q. In the process of creating the defect, that particular atom increased its energy by an amount

$$\delta E = E_c - E_q \tag{4}$$

The sum of similar contributions from the other atoms surrounding the defect amounts to the total energy necessary to create the defect.

In order to determine the equivalent lattice constant a_Q, we solve a simple transcendental equation where the only input is given by the atomic positions of the surrounding neighbors, thus carrying all the relevant information about the nature of the defect. This equation, which in what follows will be referred to as the ECT perturbation equation, results from a simple parameterization of an exact perturbative treatment of the problem:

$$N_1(c_1 a_Q)^p \exp(-\alpha c_1, a_Q) + N_2(c_2 a_Q)^p$$

$$\exp\left[-\left(\alpha + \frac{1}{\lambda}\right)c_2 a_Q\right] = \sum_j r_j \exp - [\alpha + S(r_j)]R_j \tag{5}$$

with

$$S(r_j) = \frac{1}{2\lambda}\left(1 - \cos\left[\frac{\pi(r_j - c_1 a_e)}{(c_2 - c_1)a_e}\right]\right) \tag{6}$$

where r_j stands for the distance between the jth neighbor and the atom under consideration; N_1 and N_2 are the number of nearest and next-nearest neighbors in a perfect (equivalent) crystal; $p = 2n - 2$, where n is the principal atomic quantum number; λ is the electronic screening length; α is a parameter computed by requiring agreement with the experimental vacancy formation energy; and c_1 (c_2) is the ratio between the nearest (next-nearest) neighbor distance and the lattice parameter. The sum on the right side of equation (5) is over the neighbors of the atom in the defect crystal. Once equation (5) is solved with respect to the equivalent lattice constant a_Q, the change in energy is found from the universal binding energy relation:

$$E = E_c[1 - (1 + a_Q^*)\exp(-a_Q^*)] \tag{7}$$

where

$$a_Q^* = \frac{c_1(a_Q - a_e)}{l}$$

E_c is the cohesive energy, and c_1 is the ratio between the equilibrium Wigner-Seitz radius and the lattice parameter. This procedure is performed for each atom that defines the defect and the sum of these energies represents the energy of forming the defect.

A complete formulation of ECT can be found in reference 4, where additional terms dealing with bond length anisotropy, bond angle anisotropy, and face diagonal anisotropy are included. Including these terms does not change the essence of the method, which is based on the existence of an equivalent crystal for which the brief summary included here suffices. For simplicity, we will not refer to these terms when dealing with the extension of ECT to alloys, but it must be understood that in any practical application, a full ECT treatment of the defect should be carried out following the prescription in reference 4.

Formalism

General Considerations

In order to fix these ideas, we will describe the ensuing formalism with reference to the following example. Consider two pure single crystals: one of atomic species A (lattice parameter a_e^A) and one of atomic species B (lattice parameter a_e^B). This will be the *initial state*. The *final state* will be a certain alloy AB with lattice parameter a_x. The ideal process of alloy formation is shown in figure 4.

Let us focus on one of the atoms in the A crystal. Figure 5 represents the transformation undergone by this atom. There is a change in geometry (the lattice parameter changed from a_e^A to a_x) and a change in composition (some of the neighbors are changed to B atoms, denoted by dots). As discussed above, we will break up this transformation into two independent transformations, as shown in figure 6.

In the first transformation, the identity of the atoms is conserved. The atom in question (denoted in figs. 5 and 6 by ⊗) sees its environment changed only in terms of the relative distances of the atoms surrounding it. This is a defect that can be straightforwardly treated with the current ECT

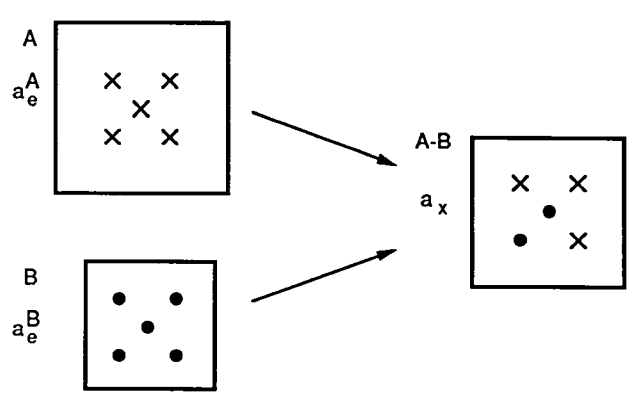

Figure 4.—Ideal process of alloy formation.

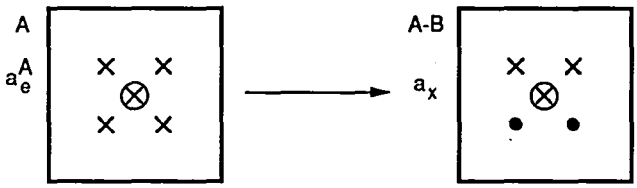

Figure 5.—Transformation of atom A in crystal.

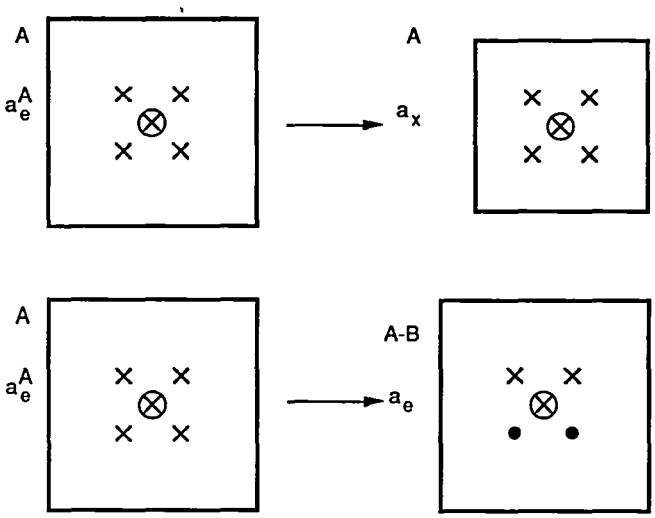

Figure 6.—Breakup of transformation shown in figure 5 into two independent transformations.

without reference to alloy formation. The atom suffers a change in energy, e_s^A, which we will call from now on strain energy, because it is related only to lattice deformations. The change in energy is simply

$$e_s^A = E_c^A[1 - (1 + a_s^*) \exp(-a_s^*)] \tag{8}$$

where

$$a_s^* = \frac{a - a_e^A}{l_A}$$

and where a is the lattice parameter of the equivalent crystal of the atom in question, which can be easily obtained by applying single-crystal ECT. The parameters E_c^A, a_e^A, and l_A are the cohesive energy, equilibrium lattice parameter, and scaling length, respectively.

In the second transformation, the geometry of the equilibrium crystal is conserved. The atom in question sees its environment changed only in terms of the identity of its neighbors. This change in energy, which we call the chemical energy, is given by

$$e_c^A = s_A E_c^A[1 - (1 + a_A^*) \exp(-a_A^*)] \exp(-a_A^*) \tag{9}$$

where

$$a_A^* = \frac{a_E - a_e^A}{l_A}$$

$s_A = +1$ if $a_A^* > 0$, $s_A = -1$ if $a_A^* < 0$, and a_E is obtained by solving a transcendental equation that will be discussed later.

The last term in equation (9) is introduced to compensate for the fact that the chemical energy, as defined here, is independent of the structure of the crystal. Without it, the chemical energy would be a constant, solely dependent on chemical composition, regardless of the relative positions of the atoms. It will be shown later that we must include this term in order to properly account for the asymptotic behavior of the enthalpies of formation of alloys. However, it will also be shown that for the description of equilibrium properties of the alloys, there is a certain arbitrariness concerning the definition of this term as well as its need altogether.

Strain Energy

The calculation of the strain energy is straightforward, as it only requires the knowledge of the location of the occupied sites surrounding the atom being studied. The first step involves solving the ECT perturbation equation for that atom in order to determine the equivalent lattice parameter a:

$$NR_1^p \exp(-\alpha R_1) + MR_2^p \exp\left[-\left(\alpha + \frac{1}{\lambda}\right)R_2\right] = \sum_i r_i^p \exp[-(\alpha + S(r_i))r_i] \tag{10}$$

where

$$S(r) = \frac{1}{2\lambda}\left(1 - \cos\left[\frac{\pi(r - R_1^o)}{(R_2^o - R_1^o)}\right]\right) \tag{11}$$

for

$$R_1^o = c_1 a_e \quad \text{and} \quad R_2^o = c_2 a_e \tag{12}$$

where r_i is the distance between the ith neighbor and the atom under consideration and N (M) is the number of (next) nearest neighbors in the perfect crystal. Also,

$$R_1 = c_1 a \quad \text{and} \quad R_2 = c_2 a \tag{13}$$

where c_1 (c_2) is such that R_1 (R_2) is the (next) nearest neighbor distance in the perfect crystal. Once the equivalent

lattice parameter a is known, the strain energy is easily computed using equation (8).

Chemical Energy

In the single-crystal ECT, where all the atoms are of the same atomic species, we apply perturbation theory in order to find the energy of the defect crystal. The perturbation is basically due to the difference in potentials between the defect solid and the ground-state crystal. As described in the original formulation of the method, it is reasonable to parameterize the first-order contributions to the perturbation expansion as

$$\Delta E \propto R^p \exp(-\alpha R) \tag{14}$$

where $p = 2n - 2$ (where n is the atom principal quantum number) and α is a parameter that will primarily reflect the structure of the electron density in the overlap region. In single-crystal ECT the parameter α is determined for metals so that the energy to form a rigid (or unrelaxed) vacancy is equal to the experimental value.

To a good approximation, these concepts should remain valid in the case of alloys, and we will adopt the same functional form used in equation (6) to describe the perturbation due to the dissimilar atomic species. In order to deal with arbitrary defects and structures in future applications, as well as with multicomponent systems, it is convenient to "localize" this effect and assume that the global property parameterized by α (i.e., the tails of the overlapping electron densities) can be separated into pairs of interacting atoms. In this approximation, the electron density in the region between two atoms of the same species would be unaffected by the presence of neighboring atoms of a different species. The perturbation would then be localized in the region between two dissimilar atoms. This assumption enables us to define the parameter α_{AB} as

$$\alpha_{AB} = \alpha_A + \Delta_{BA} \tag{15}$$

where α_A is the α value for the pure metal A and Δ_{BA} is a correction introduced by the presence of a neighbor of species B. The use of α_{AB} in the ECT will be described later. Obviously, $\Delta_{AB} = 0$ if A = B.

The "perturbation" parameters Δ_{AB} and Δ_{BA} are the only new parameters introduced in this theory of alloys, and they will be determined by fitting to appropriate experimental data.

The main ingredient in the calculation of e_c (see eq. (9)) is a_E, the equivalent lattice parameter for the atom embedded in the alloy. As noted earlier, the concept of defect, as defined in the ECT framework, is not applicable in this case: even when a single impurity is introduced in an otherwise perfect crystal, every single neighboring host atom has access to a range of atomic states that cannot necessarily be reproduced by an equivalent perfect crystal of a single species. If we were able to map the perfect crystal with the single impurity onto a homogeneous crystal where its constituents are quasiatoms that properly model the chemical composition of the impure crystal, then any alteration in the composition could be studied by recourse to a single set of equivalent crystals of the quasiatoms. This requires the *a priori* knowledge of the properties of this quasicrystal; however, these are the properties that we wish to predict. Further, the quasiatom approach makes the calculation of the energetics of an arbitrary defect, both in composition and geometry, impractical. Therefore, we are attempting to develop a method that retains the simplicity of the original ECT, where the identity of the individual constituents is maintained. We must, then, work with the framework of single crystals, where an atom of certain species is only "allowed" to have equivalent crystals of its own species, whether it is a pure environment of atoms of the same element or not.

To distinguish the type of equivalent crystals one determines when computing strain energies, we will call these new, approximate equivalent crystals, which represent solely the changes in atomic compositions, "virtual crystals." We must, of course, remember that that they are just a tool to help us approximate the "jump" into the otherwise inaccessible family of curves of the real equivalent crystals of the previously defined quasiatoms.

In order to compute the net change in chemical energy ($|e_c|$) in such a transformation (see fig. 6(b)), we first find the virtual crystal of the atom under consideration, where the defect crystal is the equilibrium crystal whose constituents are a mixture of atoms of different species.

As an example, let us consider an atom of species A which, in its reference state, would be located in a lattice site with N (M) nearest (next-nearest) neighbors. The change in composition to that of the alloy can be represented as the flipping of some of the surrounding A atoms into B, C,..., etc., atoms. When writing the ECT perturbation equation for the host atom, we distinguish each interaction by means of the coefficients $\alpha_{Aj}(j = \mathrm{B,C,...})$, such that

$$NR_1^{p_A} \exp(-\alpha_A R_1) + MR_2^{p_A} \exp\left[-\left(\alpha_A + \frac{1}{\lambda_A}\right)R_2\right] = \sum_j r_i^{p_A} \exp - [\alpha_{Aj} + S(r_i)]r_i \tag{16}$$

for

$$R_1 = c_1 a_E \quad \text{and} \quad R_2 = c_2 a_E$$

where j denotes the identity of the neighbor of atom i located at a distance r_j of the host atom and where

$$r_i \propto a_e^A \tag{17}$$

Once a_E is known, the net change in energy is obtained by means of the universal expression:

$$e_c^a = s_a E_c^a [1 - (1 + a_A^*) \exp(-a_A^*)] \exp(-a_s^*) \quad (18)$$

where

$$a_A^* = \frac{a_E - a_e^A}{l_a}$$

with $s_A = +1$ if $a_A^* > 0$ and $s_A = -1$ if $a_A^* < 0$, where a_e^A is the equilibrium lattice parameter of a pure A crystal.

The origin of the sign s_A, which obviously accounts for the direction of the energy change in the alloy, can be explained with reference to a simple model of vacancy formation, as follows: Consider a perfect A crystal which undergoes an ideal transformation where a vacancy is created without relaxation of the atomic positions of the neighboring atoms. This ideal process is shown in figure 7, where the circle denotes the vacancy site and where x denotes one of its nearest neighbors.

Each ⊗ atom increases its energy by an amount e_v, which can be easily computed with ECT. The equivalent crystal of each ⊗ atom (lattice parameter a_v), is then an expanded version of the ground-state crystal (lattice parameter a_e^A). This process, in terms of equivalent crystals, is shown in figure 8. The ideal process of creating a vacancy can be interpreted as the uniform expansion of the corresponding equivalent crystals of each one of the neighboring atoms. And the total change in energy of the defect crystal is just the sum of the energies involved in each one of these expansions.

Consider now a second, ideal, process, which is just the reverse of the process described before; that is, the vacancy is now filled, returning the defect crystal to its original state (as shown in fig. 9).

Regardless of the intermediate states reached during this process, the net result is the lowering of the energy of the system to its original value. In terms of equivalent crystals, the equivalent crystal of each neighboring atom of the vacancy undergoes a uniform compression until the lattice parameter of the equivalent crystal exactly coincides with the equilibrium lattice parameter. If we focus our attention on the initial and final states ((1) and (3) in fig. 9), there is no net change in the equivalent lattice parameter, which amounts to no net change in the energy of the crystal. The process of filling the vacancy, then, is a process that lowers the energy by an amount proportional to the reduction in the equivalent lattice parameter. If it reduces to the equilibrium value, the net change is zero.

As noted before, no exact statement can be made (in terms of equivalent crystals) with respect to a similar process where the vacancy is filled with an impurity atom, as shown in figure 10. The equivalent crystal of ⊗ in the final state (3) can be taken just as an *approximation* to the real final state (upper line in fig. 10). The process of filling the vacancy with an atom

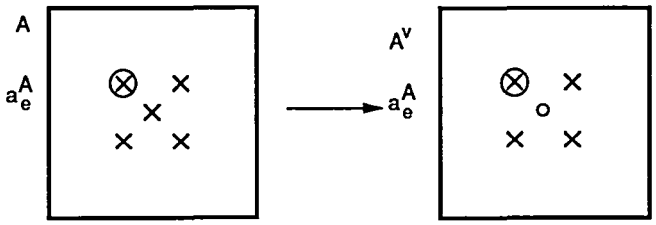

Figure 7.—Perfect crystal A undergoing ideal transformation.

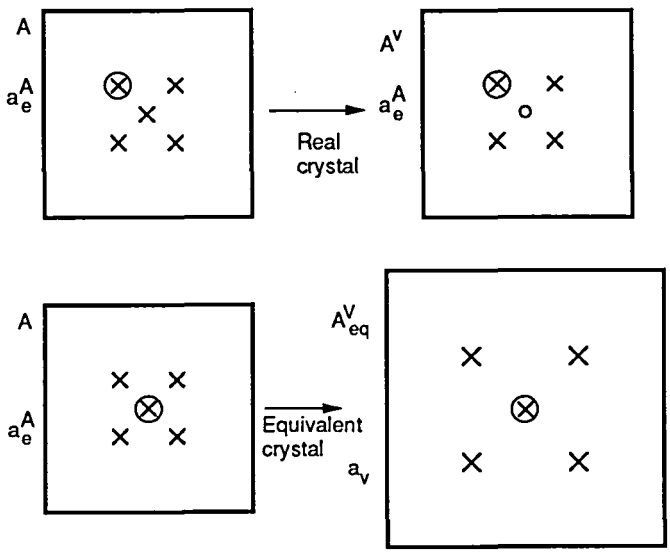

Figure 8.—Ideal process of filling a vacancy.

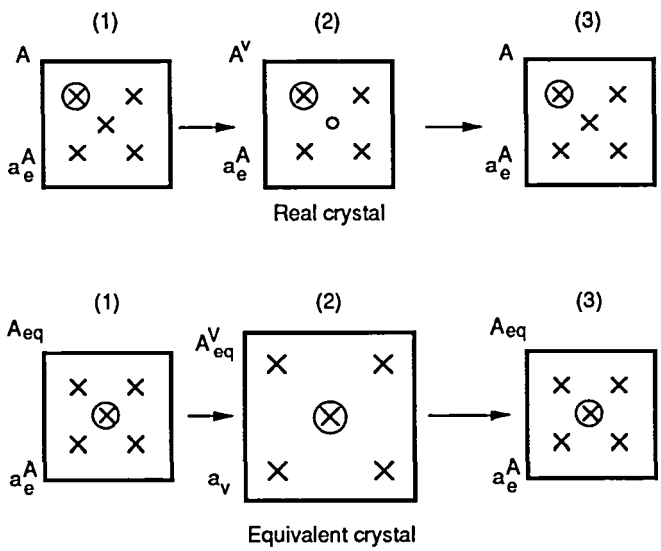

Figure 9.—Reverse of the process in figure 8.

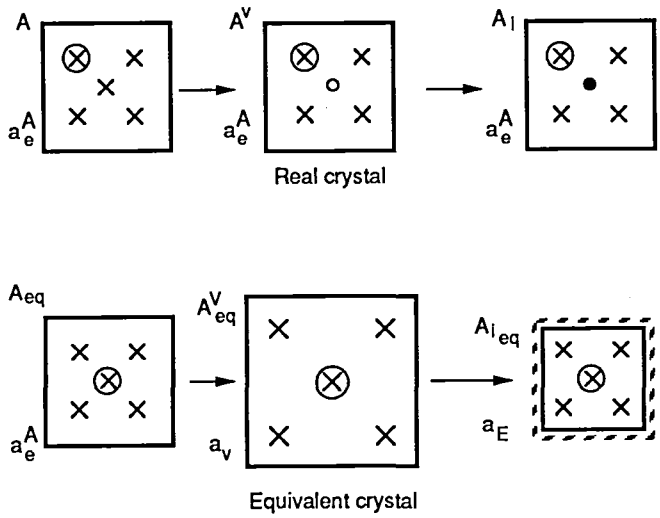

Figure 10.—Ideal process where vacancy is filled with impurity atom.

(of the species of the host or any other atomic species) is then a process which lowers the energy of the original crystal. If the lattice parameter of the equivalent crystal is greater than the equilibrium value, the *net* change is still positive, but, if it is smaller than the equilibrium value, the net change is then negative. Again, this is only an approximation, and its validity will be tested by several applications of the method.

Finally, the last term in the chemical energy equation, $e^{-a_s^*}$ (see eq. (9)), is introduced to compensate for the information lost when breaking up the process of formation of the alloy from its pure constituents into two independent processes (as shown in fig. 6). This term is proportional to the lattice parameter mismatch of the constituents. Its main role, as noted earlier, is to properly account for the asymptotic behavior of the excess energy in the formation of the alloy from its constituents, but it is almost of no relevance in the region of interest (when the typical distances in the alloy are comparable to the distances in the equilibrium metals).

Determining Δ_{AB} and Δ_{BA}

In order to fix the perturbative parameters Δ, we will use the experimental values for the heat of solution (in the dilute limit). Let's call E^{BA} the heat of solution of an impurity B in a host A. This quantity is defined as

$$E^{BA} = \left.\frac{d\Delta H}{dx}\right|_{x\to 0} \tag{19}$$

where ΔH is the heat of formation of the compound $A_{1-x}B_x$, x being the concentration of B atoms. Correspondingly,

$$E^{AB} = \left.\frac{d\Delta H}{dx}\right|_{x\to 1} \tag{20}$$

The heat of formation ΔH is defined as the difference in energy between the constituent atoms of the compound at equilibrium and their composition-averaged bulk values in the pure crystals. Later in this section, we will provide an algorithm for the calculation of ΔH.

Equations (19) and (20) form a system of two coupled equations that are solved with respect to Δ_{AB} and Δ_{BA}. Consider a binary alloy A-B on a lattice of fixed symmetry. We first compute the excess internal energy ΔE for some ordered alloys in reference to its phase separation limit. For the ordered structures, we first consider the case of a face-centered-cubic (fcc) lattice. If we assume that only clusters consisting entirely of nearest neighbors are important, then we only deal with structures of the form A_mB_{4-m} (where the largest cluster of nearest neighbors is a tetrahedron as shown in fig. 11).

These clusters are the building blocks of the corresponding ordered fcc alloys A_mB_{4-m} (see fig. 12). The excess internal energy for the ordered alloy per atom is written as

$$\Delta E_m(r) = E_m(r) - \frac{m}{4}E_4(a_e^A) - \left(1 - \frac{m}{4}\right)E_o(a_e^B) \tag{21}$$

where a_e^A and a_e^B are the equilibrium lattice constants of pure A and B metals, and $E_o(a_e^B)$ and $E_4(a_e^A)$ are the cohesive energies E_c^B and E_c^A, respectively. With these definitions, $E_m(r)$ represents the binding energy curve of the ordered alloy.

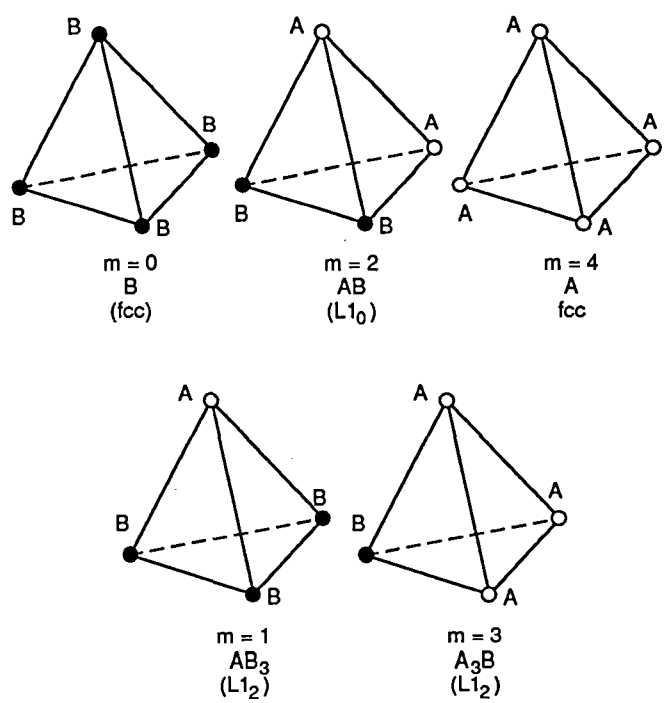

Figure 11.—Cluster of nearest neighbors.

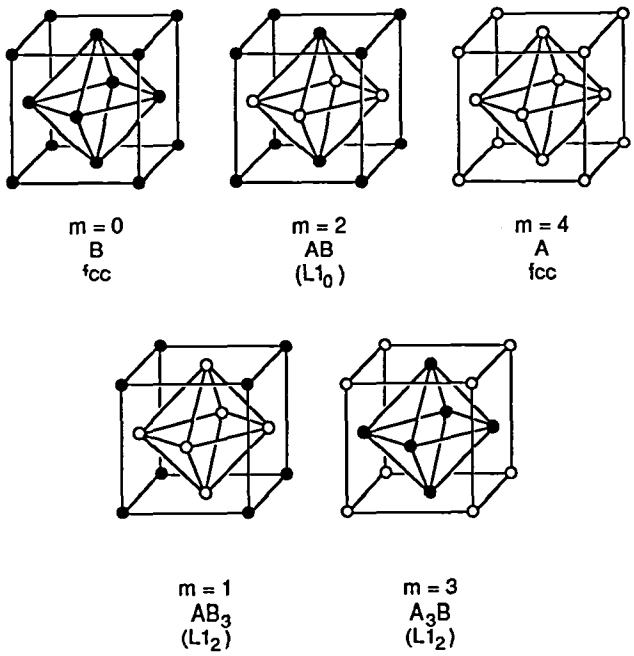

Figure 12.—Ordered fcc, A_mB_{m-4} alloy structures.

To compute $\Delta E_m(r)$ using the method described in previous sections, let us consider a compound A_mB_{4-m}, where the elementary structure contains N_A atoms of type A and N_B of type B, arranged in such a way that each one of the A atoms has N_{AA} (M_{AA}) (next) nearest neighbors of type A and N_{AB} (M_{AB}) (next) nearest neighbors of type B. The B atoms have, each, N_{BB} (M_{BB}) (next) nearest neighbors of type B and N_{BA} (M_{BA}) (next) nearest neighbors of type A. The strain energy for each A atom is

$$e_s^A(r) = E_c^A[1 - (1 + a_{sA}^*)\exp(-a_{sA}^*)] \quad \text{for } a_{sA}^* = \frac{r - a_e^A}{l} \tag{22}$$

and for each B atom is

$$e_s^B(r) = E_c^B[1 - (1 + a_{sB}^*)\exp(-a_{sB}^*)] \quad \text{for } a_{sB}^* = \frac{r - a_e^B}{l} \tag{23}$$

The chemical energy for each A atom is

$$e_c^A(r;m) = s_A E_c^A[1 - (1 + a_A^*)\exp(-a_A^*)]\exp(-a_{sA}^*) \quad \text{for } a_A^* = \frac{a_A - a_e^A}{l_a} \tag{24}$$

where a_A is a solution of

$$\begin{aligned} NR_1^{P_A}\exp(-\alpha_A R_1) + MR_2^{P_A}\exp\left(-\left[\alpha_A + \frac{1}{\lambda_A}\right]R_2\right) &= N_{AA}r_1^{P_A}\exp(-\alpha_A r_1) + N_{AB}r_1^{P_A}\exp[-(\alpha_A + \Delta_{BA})r_1] \\ &\quad + M_{AA}r_2^{P_A}\exp\left[-\left(\alpha_A + \frac{1}{\lambda_A}\right)r_2\right] \\ &\quad + M_{AB}r_2^{P_A}\exp\left[-\left(\alpha_A + \Delta_{BA} + \frac{1}{\lambda_A}\right)r_2\right] \end{aligned} \tag{25}$$

for

$$R_1 = \frac{\sqrt{2}}{2}a_A \qquad R_2 = a_A \qquad r_1 = \frac{\sqrt{2}}{2}r \qquad r_2 = r \tag{26}$$

where $s_A = +1$ if $a_A < 0$, $s_A = -1$ if $a_A > 0$, and $N = 12$ (for fcc structures) and $M = 6$ are the number of nearest and next-nearest neighbors, respectively.

A similar expression to equation (24) is found for the chemical energy of the B atoms just by exchanging A ↔ B in equations (24) to (26). It is clear then that the excess energy (eq. (21)) is just

$$\Delta E_m(r) = me_A^{(m)}(r) + (4 - m)e_B^{(m)}(r) \tag{27}$$

with

$$e_a^{(m)}(r) = e_s^A(r) + e_c^A(r;m) \tag{28}$$

and

$$e_B^{(m)}(r) = e_s^B(r) + e_c^B(r;m) \tag{29}$$

As noted before, we will determine the values of Δ_{AB} and Δ_{BA} so that our final results exactly reproduce the experimental heats of solution, which should be computed for the disordered alloys A_xB_{1-x}. An easy way of obtaining the excess energy expressions for the disordered structures A_xB_{1-x} from those for the ordered ones is by following the prescription of Connolly and Williams (ref. 5), which takes advantage of the cluster expansion of Sanchez and de Fontaine (ref. 6). In this framework, the excess energy $\Delta E_m(r)$ is written in terms of many-body interaction potentials $v_n(r)$:

$$\Delta E_m(r) = \sum_n v_n(r)\xi_{nm} \tag{30}$$

TABLE I.—MULTISITE CORRELATION FUNCTIONS FOR FCC STRUCTURES

Formula	Structure	Multisite correlation function				
		ξ_0	ξ_1	ξ_2	ξ_3	ξ_4
A	fcc	1	1	1	1	1
A_3B	$L1_2$	1	½	0	−½	−1
$(AB)_2$	$L1_0$	1	0	−⅓	0	1
AB_3	$L1_2$	1	−½	0	½	−1
B	fcc	1	−1	1	−1	1

where ξ are multisite correlation functions defined on an nth order cluster, given by

$$\xi = \frac{1}{N_n} \sum_{[p_1]} \sigma_{p_1}, \ldots, \sigma_{p_n} \tag{31}$$

where σ is a spin-like variable which takes the values +1 or −1 when the lattice site p is occupied by an A or a B atom. The sum is over all n^{th}-order ($n = 0,\ldots,4$) clusters of a given type in the lattice, and N_n is the total number of such clusters. For fcc structures, the ξ's are those shown in table I.

Inverting equation (30), we obtain the following expression for the many-body potentials:

$$\nu_n(r) = \sum_{m=0}^{4} \Delta E_m(r)[\xi^{-1}]_{nm} \tag{32}$$

with

$$\xi^{-1}_{nm} = \frac{1}{16}\begin{bmatrix} 1 & 4 & 6 & 4 & 1 \\ 4 & 8 & 0 & -8 & -4 \\ 6 & 0 & -12 & 0 & 6 \\ 4 & -8 & 0 & 8 & -4 \\ 1 & -4 & 6 & -4 & 1 \end{bmatrix} \tag{33}$$

The excess energy of completely disordered alloys is estimated by

$$\begin{aligned} \Delta E_D(r,x) &= \sum_{n=0}^{4} (1-2x)^n \nu_n(r) \\ &= \sum_{n=0}^{4} (1-2x)^n \sum_{m=0}^{4} \Delta E_m(r)[\xi^{-1}]_{nm} \\ &= \sum_{m=0}^{4} c_m(x)\Delta E_m(r) \end{aligned} \tag{34}$$

where

$$c_m(x) = \sum_{n=0}^{4} (1-2x)^n[\xi^{-1}]_{nm} = \binom{4}{m} x^m (1-x)^{4-m} \tag{35}$$

The heat of formation of the ordered structures $\Delta E_m(r_m)$ is defined as the minimum value of the excess energy $\Delta E_m(r)$ (eq. (27)), which occurs for $r = r_m$, and the heat of formation of the disordered alloys $\Delta E_D(r_x,x)$ is defined as the minimum value of $\Delta E_D(r,x)$ (eq. (32)), which occurs for $r = r_x$.

For a given pair of values (Δ_{AB}, Δ_{BA}) one can evaluate the heat of formation of the disordered alloys for any arbitrary concentration x and then compare the predicted value of the derivatives at $x = 0$ and 1 with the experimental values for the heats of solution (See ref. 7 and eqs. (19) and (20)). This evaluation is, in principle, feasible but obviously impractical. Computing some selected heats of formation for some specific concentrations is clearly desirable. One choice of these selected concentrations is the set (x = 0, x = ¼, x = ½, x = ¾, x = 1). We then interpolate the intermediate values with a polynomial

$$P(x) = ax^4 + bx^3 + cx^2 + dx + e \tag{36}$$

so that

$$\begin{aligned} &P(0) = P(1) = 0 \\ &P(1/4) = \Delta E_D(r_{1/4};\ x = 1/4) = y_1 \\ &P(1/2) = \Delta E_D(r_{1/2};\ x = 1/2) = y_2 \\ &P(3/4) = \Delta E_D(r_{3/4};\ x = 3/4) = y_3 \end{aligned} \tag{37}$$

Solving this system of linear equations we obtain the coefficients:

$$\begin{aligned} a &= 64y_2 - \frac{256}{6}(y_1 + y_3) \\ b &= \frac{32}{3}(9y_1 - 12y_2 + 7y_3) \\ c &= \frac{16}{3}\left(-13y_1 + \frac{57}{4}y_2 - 7y_3\right) \\ d &= \frac{16}{3}\left(3y_1 - \frac{9}{4}y_2 + y_3\right) \end{aligned} \tag{38}$$

Finally, the heats of solution (eqs. (19) and (20)), in terms of the coefficients of this polynomial, become

$$E^{BA} = P'(0) = d$$

$$E^{AB} = -P'(1) = 16\left(\frac{1}{3}y_1 - \frac{3}{4}y_2 + y_3\right) \tag{39}$$

The parameters Δ_{AB} and Δ_{BA} are varied until equations (39) are exactly satisfied. By determining the final values of the perturbative parameters Δ_{AB} and Δ_{BA} in this fashion, one automatically determines, by recourse to equations (30) to (35), the heats of formation of all the intermediate random alloys for arbitrary values of the concentration. This determination enables us to obtain the bulk properties of all the possible alloys. The values of the relevant ECT parameters of some fcc metals, as well as the results obtained with our formalism for the possible alloys of these elements, are discussed in the next section.

TABLE III.—PERTURBATIVE PARAMETERS OBTAINED BY FITTING TO EXPERIMENTAL VALUES FOR HEATS OF SOLUTION[a]

A	B	Perturbative parameters, Å^{-1}		Heats of solution, eV/atom	
		Δ_{AB}	Δ_{BA}	E^{BA}	E^{AB}
Cu	Ag	−0.0321	−0.0394	0.39	0.25
Ag	Au	−.0311	−.0220	−.19	−.16
Cu	Au	−.0588	−.05095	−.19	−.126
Ni	Cu	.02395	−.0131	.09	.03
Al	Cu	−.0526	−.0626	−.20	−.35
Al	Ag	.0475	−.0499	.141	−.166
Al	Au	−.0501	−.0853	−.80	−1.26
Ag	Pd	−.0431	−.02033	−.289	−.108
Au	Pd	−.0439	−.0348	−.355	−.195
Cu	Pd	−.04205	−.04795	−.436	−.392
Cu	Pt	−.0568	−.0444	−.532	−.299
Ni	Pd	−.0401	−.04665	.057	−.088
Ni	Pt	−.0603	−.0529	−.282	−.330

[a]See ref. 7.

Results

We applied the formalism to several binary alloys of Ni, Cu, Al, Au, Ag, Pd, and Pt. As with previous calculations (ref. 8), in this first application we adopted the approximation that, below the melting point, the alloying energy is independent of temperature. In later efforts, we will extend our formalism to include temperature effects, as well as local relaxation effects which, for simplicity, were ignored in the present calculations. Local relaxation effects are, however, important, especially when the atomic sizes of the constituents differ greatly (ref. 8).

Before applying our formalism to defect structures, local relaxation should be incorporated, although in the present report, it would just translate into a slightly different set of values of the perturbative parameters Δ_{AB} and Δ_{BA} from the ones reported here. For completeness, table II shows the ECT parameters for the pure metals used in this calculation.

TABLE II.—EXPERIMENTAL INPUT AND COMPUTED CONSTANTS

Element	p	Screening length l	α, Å^{-1} (a)	Electronic screening length, λ	Experimental cohesive energy, E	Equilibrium lattice constant, a
Al	4	0.336	2.105	0.944	3.34	4.04
Cu	6	0.272	2.935	.765	3.50	3.61
Ag	8	0.269	3.337	.756	2.96	4.08
Au	10	0.236	4.339	.663	3.78	4.07
Ni	6	0.270	3.015	.759	4.44	3.51
Pd	8	0.237	3.612	.666	3.94	3.89
Pt	10	0.237	4.535	.666	5.85	3.92

[a]See eq. (14)

Table III gives the values of the parameters Δ_{AB} and Δ_{BA} that one obtains when applying the formalism described in the previous section. As predicted by equations (39), with these values of Δ_{AB} and Δ_{BA}, the heats of solution are exactly reproduced, as defined by equations (19) and (20). Note that although the formal definitions of equations (19) and (20) are exact, the estimates from experiment are not. They are obtained, as others have done, from a linear approximation to the slope at the minimum concentration available, which are often too high to be accurate. Our procedure allows a method of improving on this estimate. This will be treated in a later work. The excess energy curves for ordered and disordered alloys ($\Delta E_m(r)$ and $\Delta E_D(r,x)$, respectively) can be written as (see eq. (21)):

$$\Delta E_m(r) = E_m(r) + \Delta_m^\infty$$

$$\Delta E_D(r,x) = E_x(r) + \Delta_x^\infty \tag{40}$$

with

$$\Delta_m^\infty = \frac{m}{4}E_c^A + \left(1 - \frac{m}{4}\right)E_c^B \tag{41}$$

where $E_m(r)$ ($E_x(r)$) is the binding energy curve for the ordered (disordered) compound A_mB_{4-m} (A_xB_{1-x}). These functions can be accurately described with analytical forms as

$$E_m(r) = -E_c^m(1 + a_m^*)e^{-a_m^*}$$

$$E_x(r) = -E_c^x(1 + a_x^*)e^{-a_x^*} \tag{42}$$

TABLE IV.—ECT RESULTS FOR ORDERED AND DISORDERED ALLOYS

Formula	Ordered alloys, A_mB_{4-m}				Disordered alloys, A_xB_{1-x}				Experiment values		Predicted ordering energy, E_{ord}, eV
	Lattice parameter, r_m, Å	Heat formation, $\Delta E_m(r_m)$, eV	Energy reference, Δ_m^∞, eV	Cohesive energy, E_c^m, eV	Lattice parameter, r_x, Å	Heat of formation, $\Delta E_D(r_x,x)$, eV	Energy reference, Δ_m^∞, eV	Cohesive energy, E_c^x (exp), eV	Heat of formation, ΔH_{exp}, eV	Cohesive energy, E_c^x, eV	
$CuAu_3$	4.003	−0.0588	3.710	3.769	4.008	−0.0217	3.710	3.732	−0.0311	3.741	0.0371
$(CuAu)_2$	3.909	−.0818	3.640	3.722	3.918	−.0308	3.640	3.671	−.0539	3.693	0.051
Cu_3Au	3.771	−.1646	3.570	3.735	3.798	−.0277	3.570	3.598	−.0452	3.615	.1369
$CuAg_3$	3.992	0.0366	3.095	3.058	3.996	0.0537	3.095	3.041	-----	-----	0.0171
$(CuAg)_2$	3.885	.0565	3.230	3.173	3.890	0.0803	3.230	3.150	-----	-----	.0238
Cu_2Ag	3.756	.0187	3.365	3.346	3.765	.0668	3.365	3.298	-----	-----	.0488
$AlCu_3$	3.688	−0.1083	3.460	3.568	3.698	−0.0520	3.460	3.512	−0.0728	3.533	0.0563
$(AlCu)_2$	3.788	−.1012	3.420	3.521	3.799	−.0569	3.420	3.477	−.0938	3.514	.0443
Al_3Cu	3.897	−.0999	3.380	3.480	3.915	−.0378	3.380	3.418	−.0521	3.432	.0621
$NiCu_3$	3.590	0.0052	3.734	3.729	3.592	0.0083	3.734	3.726	0.0093	3.725	0.0031
$(NiCu)_2$	3.568	.0171	3.967	3.950	3.568	.0147	3.967	3.952	.0184	3.949	−.0024
Ni_3Cu	3.548	.0200	4.201	4.181	3.548	.0140	4.201	4.187	.0179	4.183	−.006
$NiPt_3$	3.857	−0.1129	5.496	5.609	3.863	−0.0587	5.496	5.555	−0.0641	5.560	0.0542
$(NiPt)_2$	3.782	−.1390	5.142	5.281	3.790	−.0752	5.142	5.217	−.0960	5.238	.0638
Ni_3Pt	3.669	−.1958	4.789	4.985	3.689	−.0545	4.789	4.843	−.0695	4.858	.1413
$NiPd_3$	3.817	−0.0493	4.064	4.113	3.822	−0.0088	4.064	4.073	−0.0123	4.076	0.0405
$(NiPd)_2$	3.738	−.0411	4.187	4.228	3.744	−.0022	4.187	4.189	−.0055	4.192	.0389
Ni_3Pd	3.639	−.0581	4.311	4.369	3.649	.0048	4.311	4.306	.0050	4.306	.0629
$CuPt_3$	3.877	−0.0891	5.262	5.351	3.879	−0.0641	5.262	5.326	−0.0723	5.334	0.025
$(CuPt)_2$	3.818	−.1502	4.675	4.825	3.825	−.0986	4.675	4.774	−.1149	4.790	.0516
Cu_3Pt	3.729	−.1970	4.087	4.284	3.747	−.0859	4.087	4.173	−.0977	4.185	.1111
$CuPd_3$	3.830	−0.1040	3.830	3.934	3.837	−0.0687	3.830	3.899	−0.0818	3.912	0.0453
$(CuPd)_2$	3.771	−.1306	3.720	3.851	3.777	−.0912	3.720	3.811	−.1109	3.831	.0394
Cu_3Pd	3.693	−.1387	3.610	3.749	3.706	−.0728	3.610	3.683	−.0926	3.703	.0659
$AuPd_3$	3.933	−0.0597	3.900	3.960	3.935	−0.0429	3.900	3.943	−0.0476	3.948	0.0168
$(AuPd)_2$	3.975	−.0966	3.860	3.957	3.979	−.0667	3.860	3.927	−.0807	3.941	.0299
Au_3Pd	4.018	−.1061	3.820	3.926	4.026	−.0579	3.820	3.878	−.0746	3.895	.0482
$AgPd_3$	3.921	−0.0330	3.695	3.728	3.921	−0.0303	3.695	3.725	−0.0273	3.722	0.0030
$(AgPd)_2$	3.954	−.0761	3.450	3.526	3.959	−.0523	3.450	3.502	−.0520	3.502	.0238
Ag_3Pd	4.000	−.0956	3.205	3.301	4.011	−.0471	3.205	3.252	−.0524	3.257	.0485
$AlAu_3$	4.075	−0.3155	3.463	3.778	4.075	−0.2068	3.463	3.670	−0.2723	3.735	0.1087
$(AlAu)_2$	4.070	−.3054	3.316	3.621	4.070	−.2434	3.316	3.559	−.3499	3.666	.0620
Al_3Au	4.062	−.2006	3.286	3.487	4.062	−.1636	3.286	3.450	−.2095	3.495	.037
$AlAg_3$	4.072	−0.0420	3.055	3.097	4.077	−0.0160	3.055	3.071	-----	-----	0.0260
$(AlAg)_2$	4.074	.0000	3.15	3.15	4.073	−.0018	3.150	3.152	-----	-----	−.0018
Al_3Ag	4.073	.0342	3.245	3.211	4.067	.0127	3.245	3.232	-----	-----	−.0215
AgAu	4.079	−0.0401	3.535	3.575	4.079	−0.0307	3.535	3.566	−0.0341	3.569	0.0094
(AgAu)	4.081	−.0550	3.315	3.370	4.081	−.0425	3.315	3.357	−.0482	3.363	.0125
Ag_3Au	4.083	−.0475	3.117	3.165	4.083	−.0335	3.117	3.150	−.0372	3.154	.0140

where

$$a_m^* = \frac{r - r_m}{l_m} \quad \text{and} \quad a_x^* = \frac{r - r_x}{l_x}$$

In the equations E_c^m (E_c^x) is thus the cohesive energy of the ordered (disordered) alloy, and r_m (r_x) is the equilibrium lattice parameter. This result is in agreement with previous attempts to represent the binding energy curves for alloys. Moreover, equation (34) implies that

$$E_x(r) = \sum_m c_m(x) E_m(r) \tag{43}$$

and

$$\Delta_x^\infty = \sum_m c_m(x) \Delta_m^\infty \tag{44}$$

so that only the knowledge of E_c^m, a_m, l_m, and Δ_m^∞ is required, as the quantities E_c^x, r_x, l_x, and Δ_x^∞ can be obtained from equations (43) and (44). These results are listed in table IV for some of the binary alloys studied. Table IV also gives the predicted values for the heats of formation of ordered and disordered structures, as well as the experimental values. Finally, table IV includes the ordering energy, defined as

$$E_{ord}^{(m)} = \Delta E_d(r_x, x) - \Delta E_m(r_m) \tag{45}$$

for $x = m/4$ and $m = 0, 1, 2, 3, 4$.

In figure 13 we show a particular case, the $L1_0$ structure of the Ag-Pd alloy. This figure highlights the relative contributions of the strain and chemical energies to the heat of formation $\Delta E_2(r)$. Figure 14 compares the experimental values of the heat of formation (when available) with the predicted values obtained with our formalism. In most cases, especially for those alloys where the lattice mismatch is not large, the agreement is excellent. Good results are obtained in general for all the cases studied, which include two liquids: Al-Cu and Al-Au. Figure 15 compares the experimental values of the cohesive energies of the disordered compounds with the predicted values, both in reference to the values one would obtain if Vegard's law (linear average of the pure metals cohesive energies) were valid. In all cases the agreement is excellent, even in those situations where there is noticeable departure from Vegard's law. As a final test, we compare the bulk modulus predicted by ECT with experiment and the first-principles calculations of Wei et al. (ref. 9) for the ordered compounds of Cu and Au. The results are given in table V. This is a severe test of the predictions since the bulk modulus is related to the second derivative of the binding energy curve. Again, the agreement is excellent and comparable to the first-principles results.

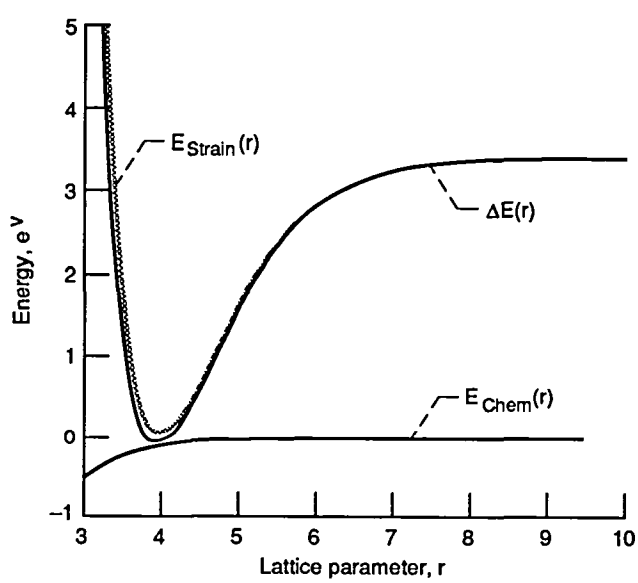

Figure 13.—Excess energy $\Delta E(r)$ of ordered compound $(AgPd)_2$ as function of lattice parameter r also showing the two contributions to excess energy $E_{strain}(r)$ and $E_{chem}(r)$.

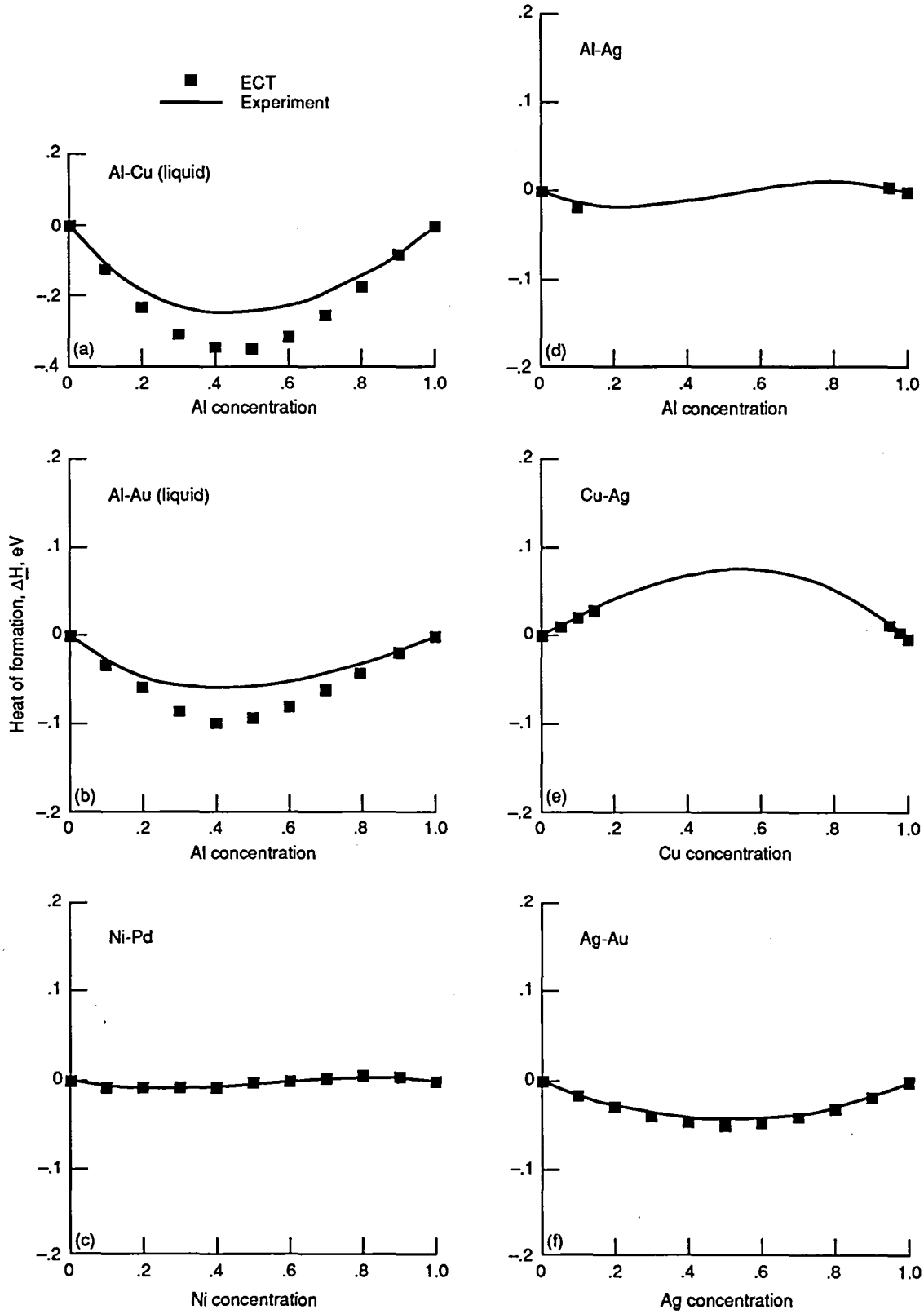

Figure 14.—Heat of formation as function of concentration

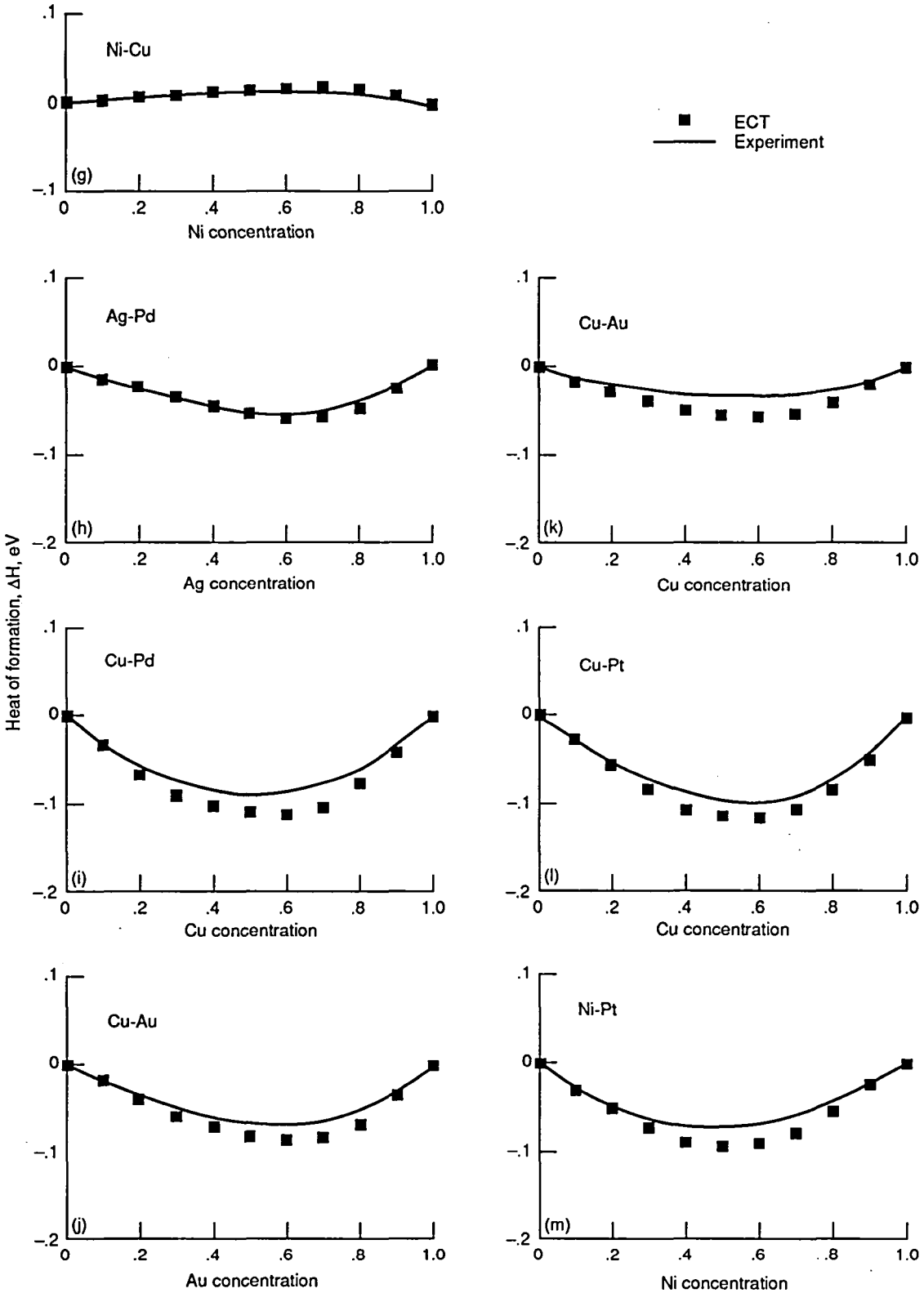

Figure 14.—Concluded.

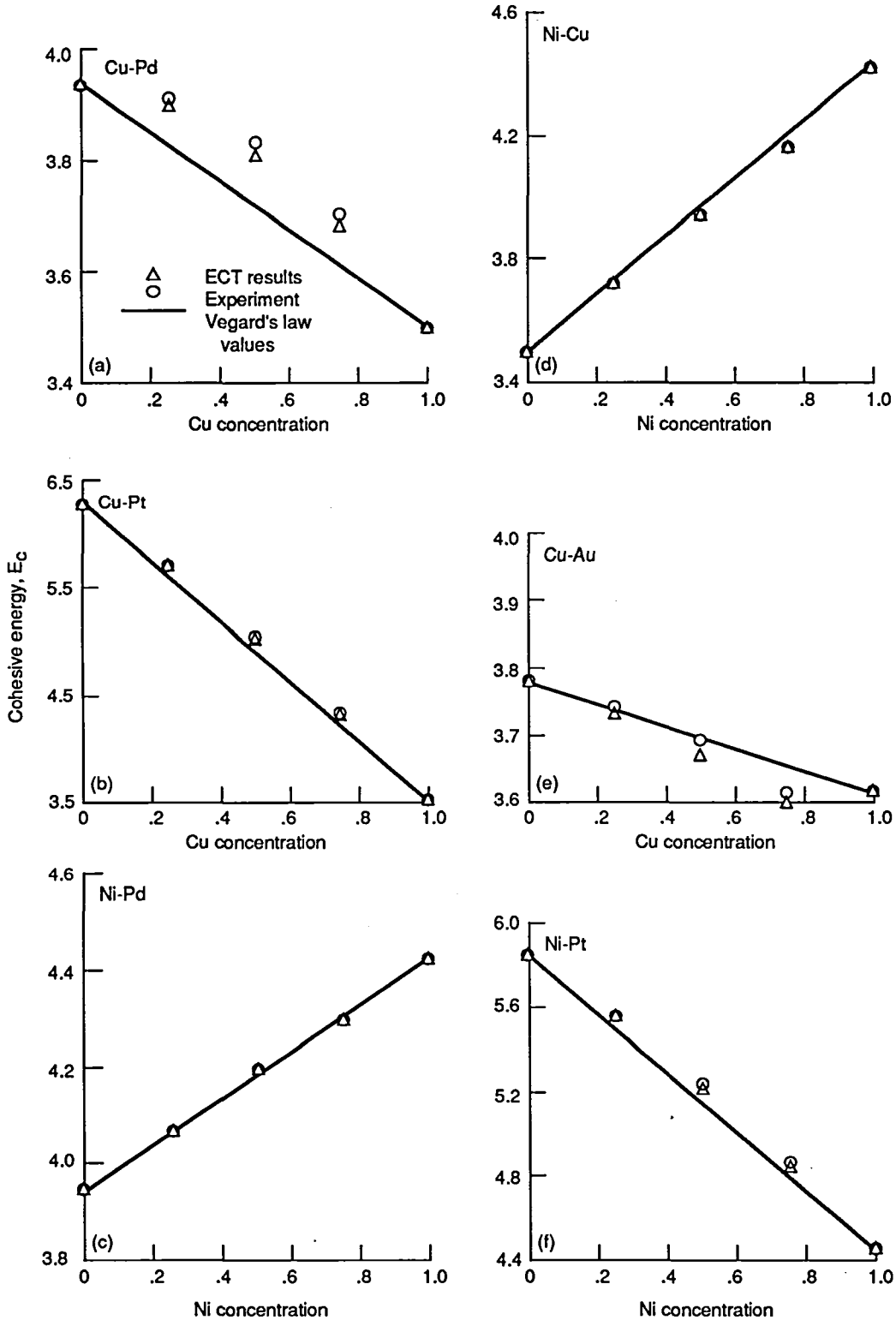

Figure 15.—Cohesive energy as function of concentration for various alloys.

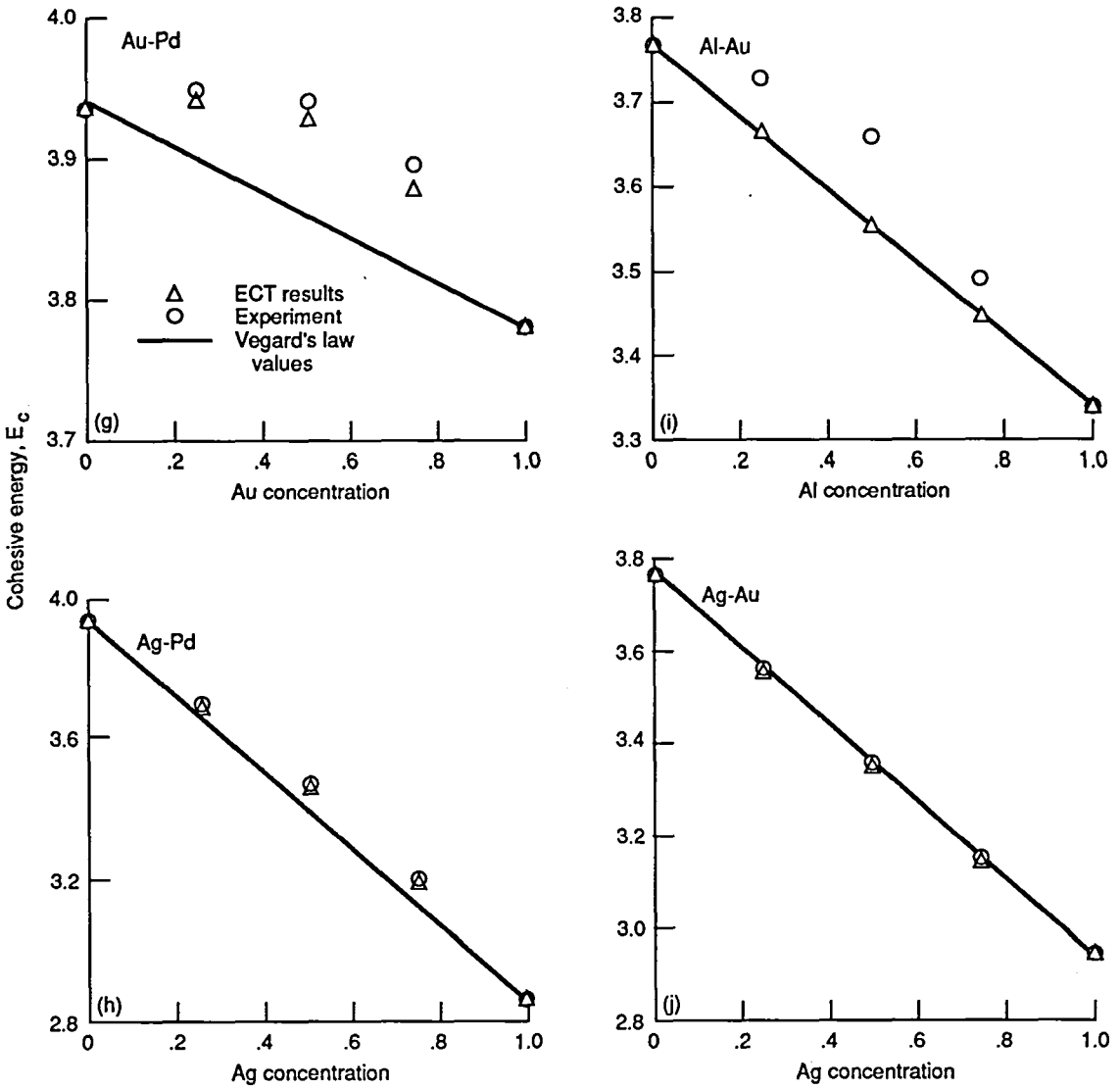

Figure 15.—Concluded.

TABLE V.—COMPARISON OF EXPERIMENTAL RESULTS, ECT PREDICTIONS, AND FIRST-PRINCIPLES CALCULATIONS (FPPL)

Formula	Type of result	Lattice parameter, a, Å	Screening length, l, Å	Cohesive energy, E_c eV	Bulk modulus, B, GPa
Cu	Experiment	3.615	0.276	3.49	138
	ECT predictions	3.615	.272	3.50	142
	FPPL	3.577	.302	4.33	144
Cu_3Au	Experiment	3.743	0.267	3.64	148
	ECT predictions	3.771	.255	3.735	165
	FPPL	3.738	.301	4.37	140
$(CuAu)_2$	Experiment	3.876	0.254	3.74	163
	ECT predictions	3.909	.246	3.722	171
	FPPL	3.887	.275	4.40	162
$CuAu_3$	Experiment	3.982	0.247	3.79	170
	ECT predictions	4.003	.240	3.769	177
	FPPL	3.991	.248	4.37	194
Au	Experiment	4.078	0.244	3.81	171
	ECT predictions	4.078	.236	3.78	181
	FPPL	·4.106	.253	4.35	180

Discussion

The results described in the previous section show how our calculations compare with the body of experimental data available, from which we extracted the information (i.e., heats of solution) needed to determine the parameters included in our theory.

In what follows, we will show how our results compare with some recent theoretical studies which include first-principles total energy calculations, based on solving the three-dimensional, nearest-neighbor, fcc Ising model with volume-dependent interaction energies, local density approximation (LDA) calculations, and embedded atom method (EAM) results (refs. 9 to 11).

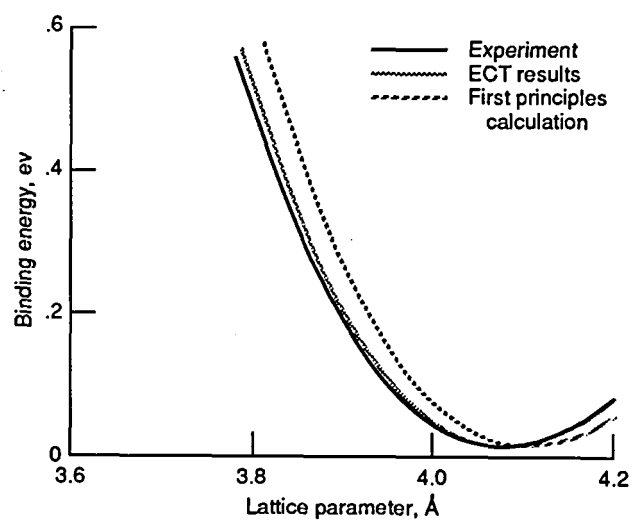

Figure 16.—Binding energy as function of lattice parameter for gold (Au). (See ref. 9.)

Comparison with First-Principles Calculations

Figure 16 shows the first of these comparisons for the particular case of Cu-Au alloys. All three sets of results for the binding energy curves of the ordered compounds A_mB_{4-m} (i.e., experimental values (EXP, ref. 7), first-principles (FPPL, ref. 9), and ECT) can be represented by simple Rydberg functions of the form

$$E_m(r) = -E_c^m(1 + a_m^*)e^{-a_m^*} \tag{46}$$

with

$$a_m^* = \frac{q}{l_m}(r - r_m)$$

where $q = (3/16\pi)^{1/3}$ for fcc only. Table V gives the values of E_c^m, r_m, and l_m for all three sets of results (EXP, FPPL, and ECT). For clarity, we first show the binding energy curves for gold in figure 16 as obtained with the parameters of table V. Figure 17 expands on these results showing the corresponding results for Cu, Au, and the three intermediate ordered compounds.

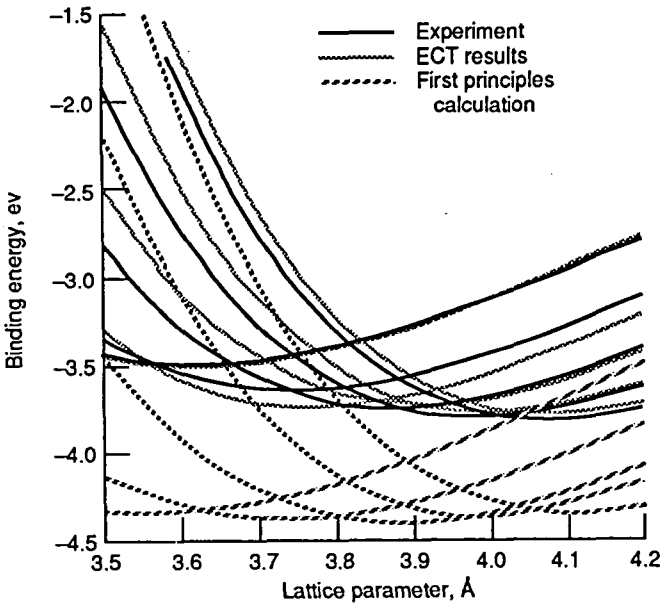

Figure 17.—Binding energy as function of lattice parameter for ordered compounds Cu_mAu_{4-m}.

Comparison with Other Semiempirical Methods.

In a recent study (ref. 11), the embedded atom method (EAM) was applied to the calculation of formation enthalpies and lattice parameters of Pd-Ni alloys. The embedding functions used were those determined for the pure metals, and the original EAM prescription was used. The comparison with experimental results is disappointing. Since then, EAM has been reformulated for alloys in order to improve the accuracy of its predictions.

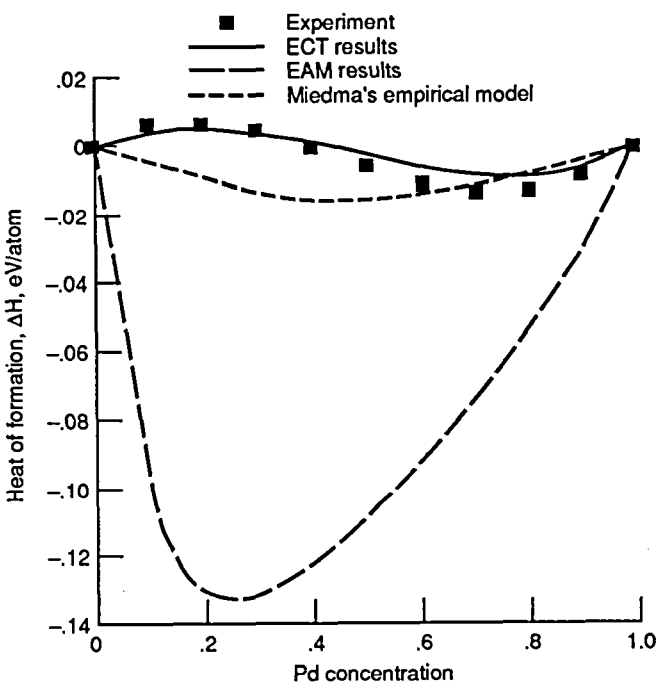

Figure 18.—Heat of formation as function of concentration for Pd-Ni alloys.

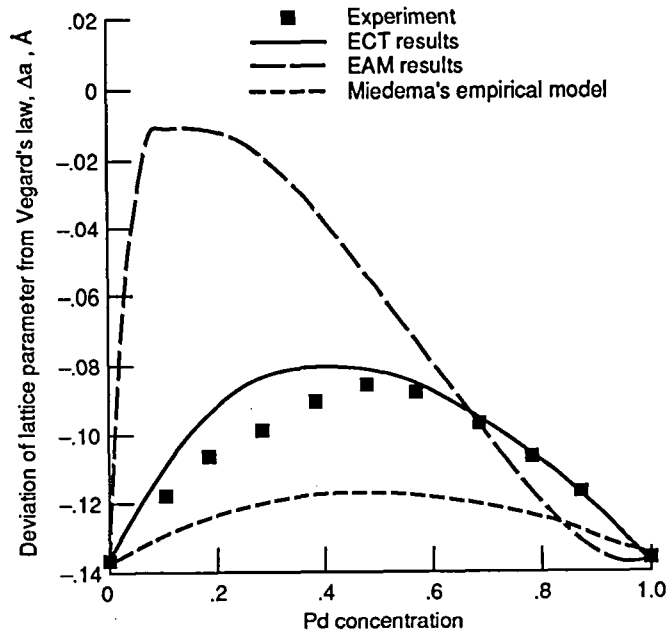

Figure 19.—Deviation from Vegard's law for lattice parameters of Pd-Ni alloys as function of concentration.

For comparison, figure 18 shows the ECT values, the EAM results, the experimental values, and the predictions of Miedema's empirical model for the formation enthalpy of the Pd-Ni alloys as a function of composition. Figure 19 shows the corresponding results for the lattice parameters.

Decoupling the Strain and the Chemical Energy

As pointed out before, our formalism is based on the assumption that the structural changes in alloy formation (strain energy) and the composition changes (chemical energy) can be treated separately. This is later corrected (in an approximate way) by introducing a geometrical factor in the expression for the chemical energy (see eq. (9)). It was later argued that in spite of the fact that this term is strictly necessary in order to ensure the correct asymptotic behavior of the formation enthalpies, it is not fundamentally important for the study of the alloy properties near equilibrium.

Not including this term in the chemical energy would effectively decouple the chemical and the strain energies leading to an approximation to what is already an approximate method. However, we will show below that this approximation leads to an interesting result concerning general properties of alloys, which in most cases can make a full calculation of alloy structure with any available method, unnecessary.

If the geometry factor in the expression for the chemical energy is left out ($e^{-a_s^*}$ in eq. (9)), the chemical energy is dependent only on chemical composition and the strain energy carries all the information about the atomic distribution and composition in the alloy. The values of the parameters Δ_{AB} and Δ_{BA} obtained are then slightly different from the ones quoted earlier, as shown in table VI, where the two sets of Δ's are listed. The ensuing results for the enthalpies of

TABLE VI.—COMPARISON OF COUPLED AND UNCOUPLED VALUES OF THE PERTURBATIVE PARAMETERS

A	A	Δ_{AB}		Δ_{BA}	
		Uncoupled	Coupled	Uncoupled	Coupled
Cu	Ag	−0.0380	−0.0321	−0.0289	−0.0394
Ag	Au	−.0311	−.0311	−.0220	−.0220
Cu	Au	−.0711	−.0588	−.0404	−.05095
Ni	Cu	.0260	.02395	−.0130	−.0131
Al	Cu	−.0415	−.0526	−.0775	−.0626
Al	Ag	.0487	.0475	−.0492	−.0499
Al	Au	−.0501	−.0501	−.0853	−.0863
Ag	Pd	−.0381	−.0431	−.0246	−.02033
Au	Pd	−.0385	−.0439	−.0411	−.0348
Cu	Pd	−.0488	−.04205	−.0413	−.04795
Cu	Pt	−.0653	−.0568	−.0367	−.0444
Ni	Pd	−.0491	−.0401	−.0376	−.04665
Ni	Pt	−.0719	−.0603	−.0431	−.0529

formation are still good and in some cases indistinguishable from the previous results. Figure 20 displays, for comparison, the original results, the new, approximate results, and the corresponding experimental values for some of the compounds studied.

As before, the results obtained for the binding energy curves of the disordered alloys, as well as the corresponding ones for the ordered alloys, can be accurately represented by simple analytical expressions:

$$\Delta E_m(r) = -E_c^m(1 + a_m^*)e^{-a_m^*} + \Delta_m^\infty;\ a_m^* = \frac{q}{l_m}(r - r_m) \tag{47}$$

$$\Delta E_D(r,x) = -E_c^x(1 + a_x^*)e^{-a_x^*} + \Delta_x^\infty;\ a_x^* = \frac{q}{l_x}(r - r_x) \tag{48}$$

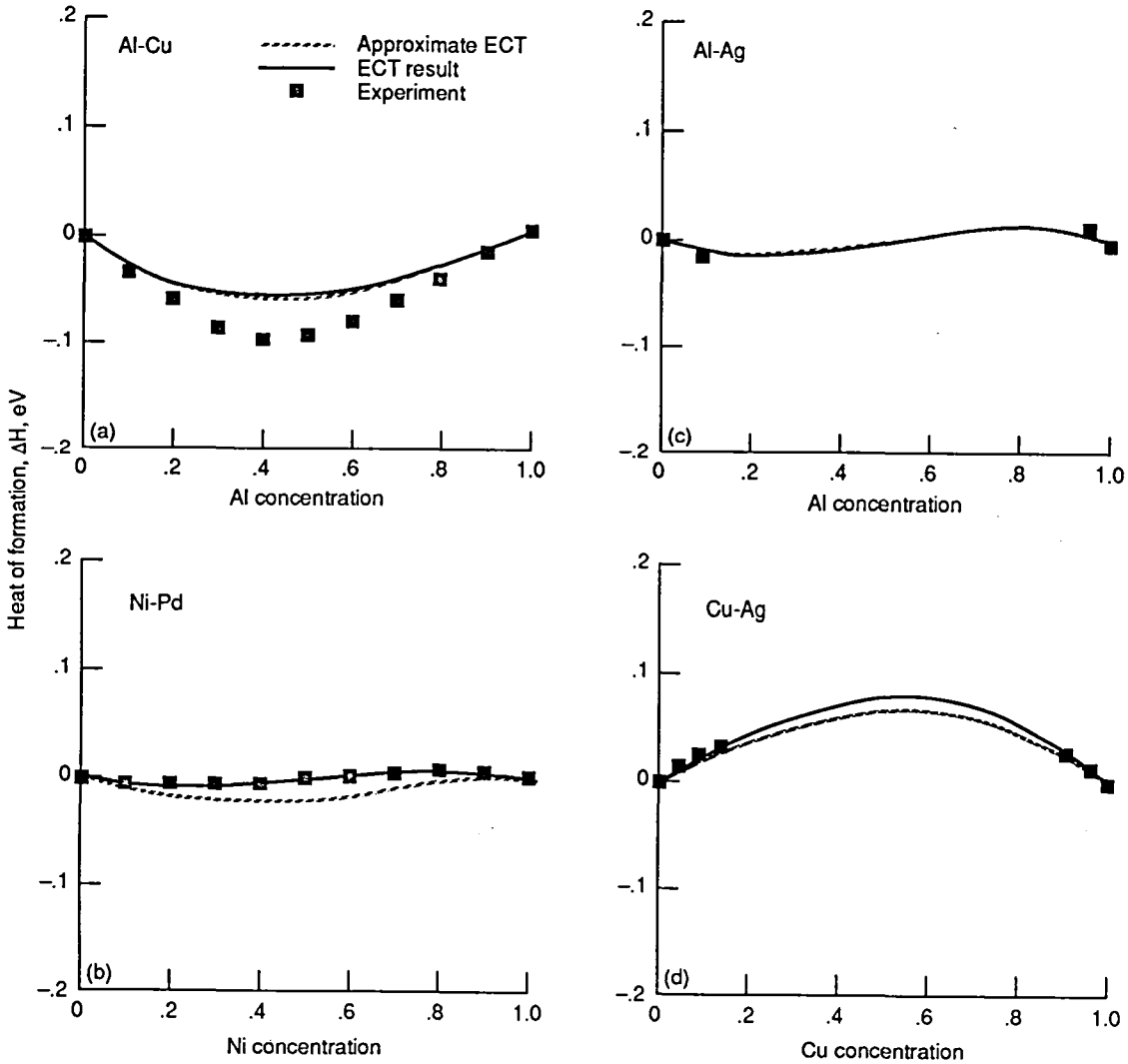

Figure 20.—Comparison of approximate ECT results and results shown in figure 14.

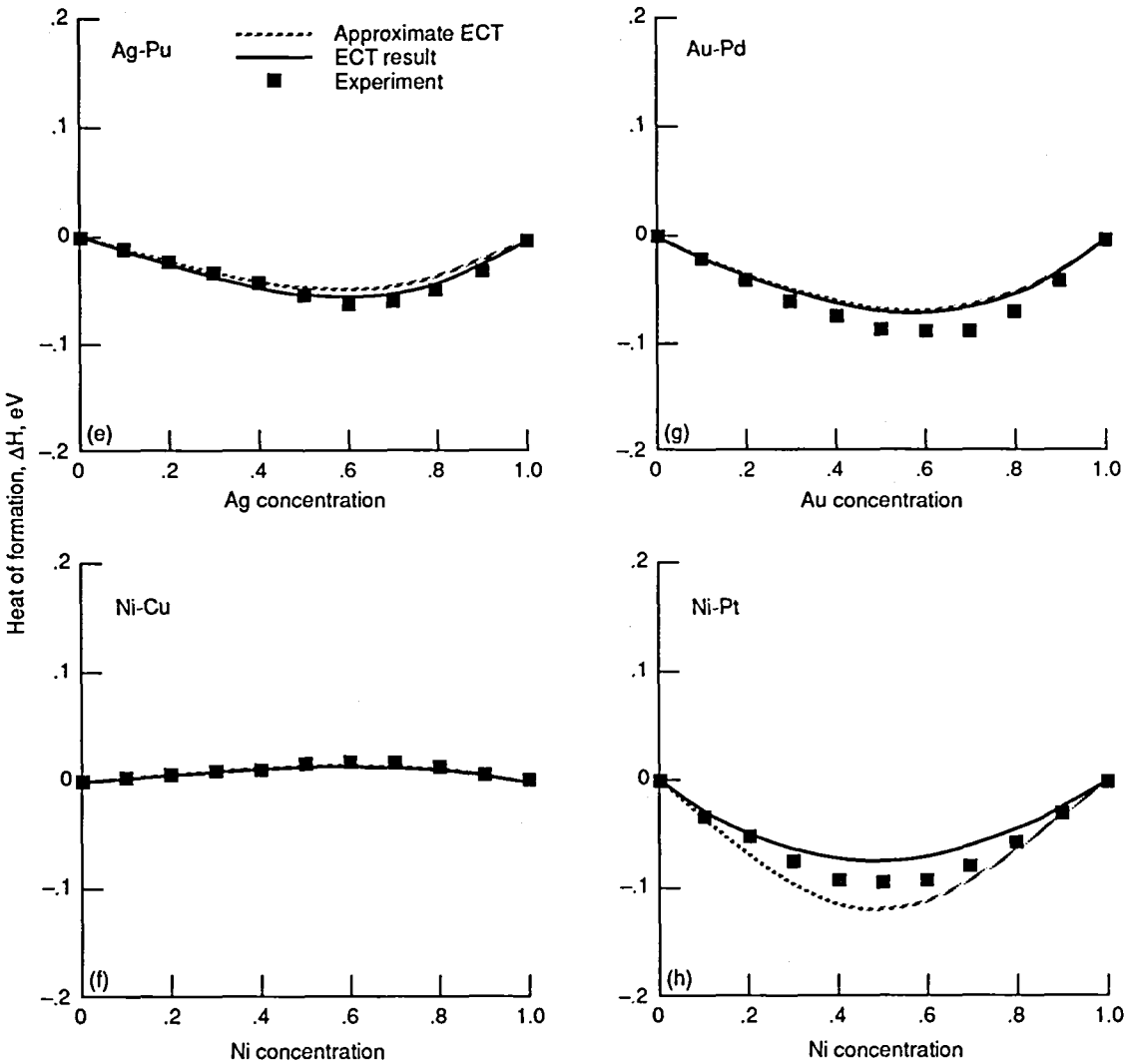

Figure 20.—Concluded.

where the quantities E_c^m, r_m, l_m, and Δ_m^∞, as well as E_c^x, r_x, l_x, and Δ_x^∞, are also different from the ones one obtains when applying the original formalism. However, in this case, the sets of values (E_c^m, r_m, l_m) and (E_c^x, r_x, l_x) are the same when $x = m/4$. This means that, apart from the reference energies Δ_m^∞ and Δ_x^∞, the binding energy curves for the disordered and ordered alloys of the same concentration coincide exactly. The only difference arises in the reference energy term.

If we insert equations (47) and (48) into equation (34), we find that two separate conditions are then satisfied:

$$\Delta_x^\infty = \sum_{m=0}^{4} c_m(x)\Delta_m^\infty \tag{49}$$

and

$$E_c^x(1 + a_x^*)\exp(-a_x^\infty) = \sum_{m=0}^{4} c_m(x)E_c^m(1 + a_m^*)\exp(-a_m^*) \tag{50}$$

These results were also valid before, but the fact that the sets of values (E_c^m, r_m, l_m) and (E_c^x, r_x, l_x) are identical when $x = m/4$ we may write equation (50) in the following fashion, reflecting the equivalence of the binding energy curves for specific concentrations (i.e., $E_x(r) = E_m(r)$ for $x = m/4$):

$$E_n(r) = \sum_{m=0}^{4} c_m\left(x = \frac{n}{4}\right) E_m(r); \qquad n = 0,\ldots,4 \tag{51}$$

Equation (51) is just a linear system of equations for $E_i(r)$, which yields the result

$$E_m(r) = \left(1 - \frac{m}{4}\right) E_o(r) + \frac{m}{4} E_4(r) \tag{52}$$

This result, which is only valid within the context of this approximation (when the strain and chemical energy are "decoupled") states that Vegard's law is valid for the binding energy curve and not just for the individual parameters in them. By virtue of equation (34), we can extend this result to the disordered alloys, obtaining

$$E_D(r,x) = (1 - x)E_o(r) + xE_4(r) \tag{53}$$

With these results, certain alloy properties can then be obtained without a full many-atom calculation. One would expect these predictions to be valid according to the relevance of the coupling between the chemical and strain energies. Figure 20 shows that, in some cases, this is an excellent approximation. The prescription for its use, therefore, is to use the UBER to generate the binding energy curves for the pure materials and then to build the alloy curve as prescribed above.

Note that this approximation is limited, not only by the underlying assumptions, but also by its inability (by definition) to reproduce the correct asymptotic behavior of the excess energy. The range of validity is thus restricted to the "local" regime, that is, when the distances involved are comparable to those in the pure metals near equilibrium.

Comparison with Other First-Principles Calculation—Test of the Sum Rule for Binding Energy Curves

In a recent calculation Terakura et al. (ref. 10) analyzed the phase stability of several binary alloy systems composed of Ni, Pd, or Pt as one element and Cu, Ag, or Au as the other. From their LDA band calculations they found that their predictions for the excess energy $\Delta E_m(r)$ admitted a simple parameterization of the form

$$\Delta E_m(r) = \left(\frac{p_m}{r}\right)^{2n} - \left(\frac{q_m}{r}\right)^{n} r_m \tag{54}$$

where the parameters p_m, q_m and r_m are those listed in table VII. They also found that a good fit was obtained for $n = 3.5$.

The objective in this section is to show that even first-principles results, to a certain extent, follow the general sum rule derived in the previous section (eq. (52)). To that effect,

TABLE VII.—FITTING PARAMETERS OF EQUATION (45)

[Ref. 10.]

System	p	q	r
Au	8.584	11.677	2.155
$CuAu_3$	8.217	11.013	1.932
$(CuAu)_2$	7.877	10.450	1.788
Cu_3Au	7.474	9.749	1.586
Cu	7.055	9.033	1.410
Ag	8.075	10.444	1.513
$CuAg_3$	7.819	10.076	1.502
$(CuAg)_2$	7.588	9.787	1.519
Cu_3Ag	7.322	9.406	1.469
$AgAu_3$	8.447	11.347	1.960
$(AgAu)_2$	8.331	11.073	1.815
Ag_3 Au	8.207	10.769	1.662

we note that in order for this rule to hold true, equation (51), together with equations (49) and (50), must be satisfied for any arbitrary choice of the parameterization of the binding energy dependence on the lattice parameter. Introducing equation (54) into equation (34), we obtain the following expression for the excess energy of the corresponding disordered compounds:

$$\Delta E_D(r,x) = \frac{P_x^{2n}}{r^{2n}} - \frac{Q_x^n}{r^n} + R_x \tag{55}$$

where

$$\begin{aligned} P_x^{2n} &= \sum_{m=0}^{4} c_m(x) p_m^{2n} \\ Q_x^n &= \sum_{m=0}^{4} c_m(x) q_m^n \\ R_x &= \sum_{m=0}^{4} c_m(x) r_m \end{aligned} \tag{56}$$

If the first-principles results behave according to equation (52), then a direct consequence of the sum rule (eq. (34)), namely,

$$\Delta E_D\left(r, x = \frac{m}{4}\right) - \Delta E_m(r) \qquad m = 0,\ldots,4 \tag{57}$$

would also have to be satisfied. In terms of the coefficients used in Terakura's work, this condition can be written as a set of simultaneous requirements on these coefficients:

TABLE VIII.—COMPARISON OF THE SETS OF PARAMETERS (P,Q,R) AND (p,q,r) AS DEFINED BY EQUATION (57)

System	P/p	Q/q	R/r
$AgAu_3$	8.46/8.45	11.37/11.35	1.98/1.96
$(AgAu)_2$	8.33/8.33	11.07/11.07	1.82/1.82
Ag_3Au	8.21/8.21	10.77/10.77	1.66/1.66
$CuAg_3$	7.84/7.82	10.11/10.08	1.51/1.50
$(CuAg)_2$	7.60/7.59	9.77/9.79	1.50/1.52
Cu_3Ag	7.34/7.32	9.42/9.41	1.46/1.47
$CuAu_3$	8.26/8.22	11.07/11.01	1.95/1.93
$(CuAu)_2$	7.91/7.88	10.45/10.45	1.77/1.79
Cu_3Au	7.52/7.47	9.78/9.75	1.59/1.59

$$P_{1/4}^{2n} = p_1 \quad Q_{1/4}^{n} = q_1 \qquad R_{1/4} = r_1$$

$$P_{1/2}^{2n} = p_2 \quad Q_{1/2}^{n} = q_2 \qquad R_{1/2} = r_2$$

$$P_{3/4}^{2n} = p_3 \quad Q_{3/4}^{n} = q_3 \qquad R_{3/4} = r_3$$

The results are shown in table VIII. Although the comparison is not exact (i.e., the (P,Q,R) and (p,q,r) coefficients are not exactly the same), the agreement is surprisingly good, making the use of equation (52) a viable alternative to Vegards's law for obtaining a more accurate and complete calculation of general alloy properties.

Conclusion

The equivalent crystal theory, originally developed for the study of pure metals and semiconductors, has been extended to include binary alloys. A simple formalism, inspired by the concept of equivalent crystals, was derived and, with minimum experimental input, applied to a large number of metallic alloys of Cu, Ni, Pd, Pt, Au, Al, and Ag. The results, which in all cases closely follow the experimental measurements of certain properties of the alloys for all ranges of compositions, compare favorable with other approaches. By construction, the method allows for a simple treatment of defects in alloys as well as extensions to include temperature effects, making this new equivalent crystal theory of alloys a versatile tool for several applications of interest.

Lewis Research Center
National Aeronautics and Space Administration
Cleveland, Ohio, April 4, 1991

References

1. Smith, J.R.; and Banerjea, A.: A New Approach to Calculation of Total Energies of Solids With Defects—Surface Energy Anisotropies. Phys. Rev. Lett., vol. 59, no. 21, 1987, pp. 2451–2454.
2. Smith, J.R.; and Banerjea, A.: Equivalent-Crystal Theory of Oscillatory Surface Relaxation. Phys. Rev., B, vol. 37, no. 17, 1988, pp. 411–414.
3. Smith, J.R., et al.: Avalanche in Adhesion. Phys. Rev. Lett., vol. 63, no. 12, 1989, pp. 1269–1272.
4. Smith, J.R., et al.: Equivalent Crystal Theory of Metal and Semiconductor Defect. To be published in Phys. Rev., B, 1991.
5. Connolly, J.W.D.; and Williams, A.R.: Density Functional Theory Applied to Phase-Transformations in Transition-Metal Alloys. Phys. Rev., B, vol. 27, no. 8, 1983, pp. 5169–5172.
6. O'Keeffe, M.; and Navrotsky, A.: Structure and Bonding in Crystals. Academic Press, 1981, Vol. 2, p. 11.
7 Hultgren, R.R: Selected Values of Thermodynamic Properties of Metals and Alloys. Wiley, 1963.
8 Ackland, G.J.; and Vitek, V.: Many-Body Potentials and Atomic-Scale Relaxations in Nobel-Metal Alloys. Phys. Rev. B, vol. 41, no. 15, 1990, pp. 10324–10333.
9 Wei, S.-H., et al.: First-Principles Calculations of the Phase-Diagrams of Noble-Metals: Cu-Au, Cu-Ag, and Ag-Au. Phys. Rev., B, vol. 36, no. 8, 1987, pp. 4163–4185.
10. Terakura, K., et al.: Electronic Theory of the Alloy Phase-Stability of Cu-Ag, Cu-Au, and Ag-Au Systems. Phys. Rev., B, vol. 35, no. 5, 1987, pp. 2169–2173.
11. Maarleveld, P.R., et al: Application of the Embedded Atom Method to the Calculation of Formation Enthalpies and Lattice Parameters of Pd-Ni Alloys. Physica, B, vol. 142, 1986, pp. 328–331.
12. Kittel, C.: Introduction to Solid State Physics. 4th ed. Wiley, 1971.

REPORT DOCUMENTATION PAGE

Form Approved
OMB No. 0704-0188

Public reporting burden for this collection of information is estimated to average 1 hour per response, including the time for reviewing instructions, searching existing data sources, gathering and maintaining the data needed, and completing and reviewing the collection of information. Send comments regarding this burden estimate or any other aspect of this collection of information, including suggestions for reducing this burden, to Washington Headquarters Services, Directorate for Information Operations and Reports, 1215 Jefferson Davis Highway, Suite 1204, Arlington, VA 22202-4302, and to the Office of Management and Budget, Paperwork Reduction Project (0704-0188), Washington, DC 20503.

1. AGENCY USE ONLY *(Leave blank)*

2. REPORT DATE
September 1991

3. REPORT TYPE AND DATES COVERED
Technical Paper

4. TITLE AND SUBTITLE
Equivalent Crystal Theory of Alloys

5. FUNDING NUMBERS
505-90-51

6. AUTHOR(S)
Guillermo Bozzolo and John Ferrante

7. PERFORMING ORGANIZATION NAME(S) AND ADDRESS(ES)
National Aeronautics and Space Administration
Lewis Research Center
Cleveland, Ohio 44135-3191

8. PERFORMING ORGANIZATION REPORT NUMBER
E-5996

9. SPONSORING/MONITORING AGENCY NAMES(S) AND ADDRESS(ES)
National Aeronautics and Space Administration
Washington, D.C. 20546-0001

10. SPONSORING/MONITORING AGENCY REPORT NUMBER
NASA TP-3155

11. SUPPLEMENTARY NOTES
Guillermo Bozzolo, Analex Corporation, 21775 Brookpark Road, Fairview Park, Ohio 44126. John Ferrante, NASA Lewis Research Center. Responsible person, John Ferrante, (216) 433-6069.

12a. DISTRIBUTION/AVAILABILITY STATEMENT
Unclassified-Unlimited
Subject Category 26

12b. DISTRIBUTION CODE

13. ABSTRACT *(Maximum 200 words)*

Equivalent Crystal Theory (ECT) is a new, semiempirical approach to calculating the energetics of solid with defects. The theory has successfully reproduced surface energies in metals and semiconductors. The theory of binary alloys to date, both with first-principles and semiempirical models, has not been very successful in predicting the energetics of alloys. This procedure, then, is used to predict the heats of formation, cohesive energy, and lattice parameter of binary alloys of Cu, Ni, Al, Ag, Au, Pd, and Pt as functions of composition. The procedure accurately reproduces the heats of formation versus composition curves for a variety of binary alloys. The results are then compared with other approaches such as the embedded atom method or Miedema's method. In addition, a new sum rule which predicts the cohesive energies and lattice parameters of alloys from pure metal properties more accurately than Vegard's law is presented.

14. SUBJECT TERMS
Alloys; Heats of formation; Cohesive energies

15. NUMBER OF PAGES
24

16. PRICE CODE
A03

17. SECURITY CLASSIFICATION OF REPORT
Unclassified

18. SECURITY CLASSIFICATION OF THIS PAGE
Unclassified

19. SECURITY CLASSIFICATION OF ABSTRACT
Unclassified

20. LIMITATION OF ABSTRACT

NSN 7540-01-280-5500

Standard Form 298 (Rev. 2-89)
Prescribed by ANSI Std. Z39-18
298-102

NASA-Langley, 1991